**California State Polytechnic University, Pomona**

**Mechanical Engineering Department**

**MEMORANDUM**

**To:** Professor McNamara **Date:** May 20, 2025

**From:** Group 3

**Members:** Isai Alcaraz, Isabella Davila, Shruthika Ilavarasu, Maghen Saltzman, Chiara Wu

**Subject**: Thermal System Design of an Electric Vehicle

## Introduction

A thermal systems design model of an electric vehicle was developed to determine the operational conditions inside the thermal management system in a typical EV car. The system consists of an 8,000-pound vehicle subject to aggressive US06 Supplemental FTP driving schedule over a 12-hour period. The vehicle has dimensions of 221" length, 84" width, 77" height. It must maintain optimal operating temperatures across all of its subsystems, while going through the drive cycle including a 10% grade ascension and descension during specific time intervals.

The thermal management subsystems include:

- Environmental Conditions Model which simulates ambient temperature variations, solar loads and fluxes, and the direction of the solar load throughout the time and travel path.
- Electric motor and gearbox Model which is a closed loop oil cooling maintaining system which maintains the temperatures to be below 100°C for the motor at 90 percent efficiency.
- The Electrical Inverter runs at an operational efficiency of 90% with IGBT cooling through a cold plate system to keep the temperatures below 125°C with the coolant inlet maintained to be below 50°C.
- Battery System which uses a 3.65 V 50.5 Ah lithium NMC pouch with cells arranged in packs with water jacket cooling to maintain temperatures below the critical temperature of 45°C, operating at 90% efficiency.
- The Cabin Interior and HVAC system which is modeled after a Ford Transit to calculate thermal loads and maintain the passengers at 70°F, while accounting for passenger heat generation and the solar loads from the environment.
- Thermal equipment and plumbing which outlines the path the coolant travels through the total model of the electric vehicle using 50% water mixture and ethylene glycol.

## Environmental Model

This system's environment is based off where the vehicle is traveling throughout the duration of its drive. It was decided that it would be traveling across the I-5 highway, starting from Los Angeles and traveling to Sacramento, then back to Los Angeles continuously, in the time frame of 12 hours from sunrise to sunset. The system's environmental conditions were modeled to be a continuous smooth curve starting and ending at the same ambient conditions and peaking in temperature in the middle of the day.

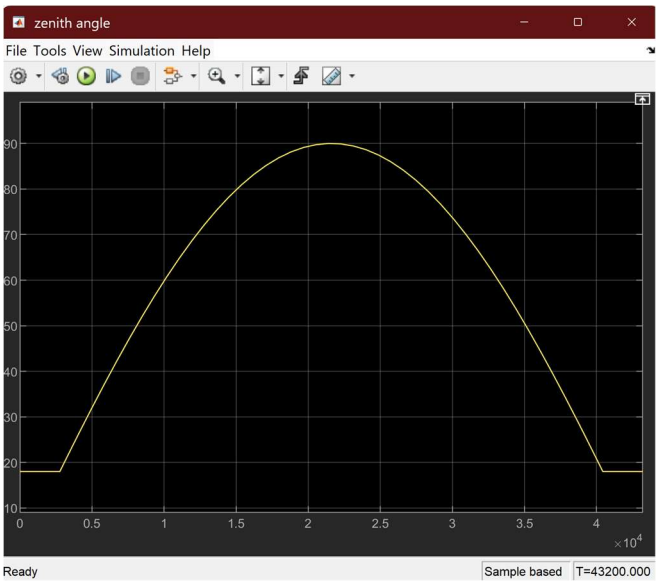


Figure 1. Sun (zenith) angle over 12 hours

The day would start with the sun rising over a slight horizon facing 20° to the electric vehicle's left side, then set 20° on the left side as well since the car would be returning to the south at the end of the day. At 12 PM when the sun is at 90° above earth, it would be directly above the car at Sacramento.

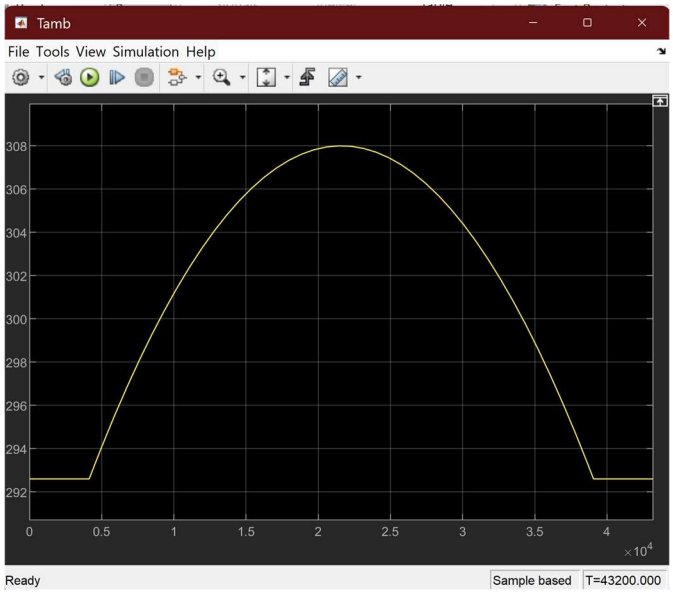


Figure 2. Ambient Temperature of the air surrounding the car

The average hottest temperatures in the most recent years (2023 and 2024) were recorded in Sacramento and Los Angeles July summers to be 85 to 95°F. The hottest temperature of 95°F in Sacramento was used, which is 35°C, or 308 K [1]. In the start of the day, it is the average low in July for Los Angeles, 67°F or 292.5 K [2]. Therefore, in accordance with the vehicle's path of

travel, it starts with the lowest temperature in Los Angeles, in the middle of the day it reaches the hottest average temperature in Sacramento, then it returns to the lowest temperature at Los Angeles at sunset. These temperatures are used to calculate the sky temperature in Figure 3.

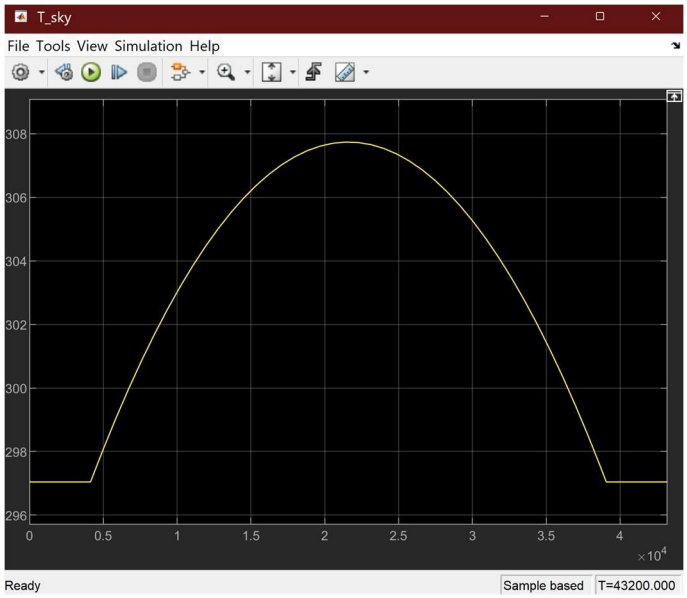


Figure 3. Sky temperature in accordance with ambient temperature

The hottest solar flux to IR was also mapped in a smooth curve, peaking at 12PM at 1414 W/m^2 in Figure 4.

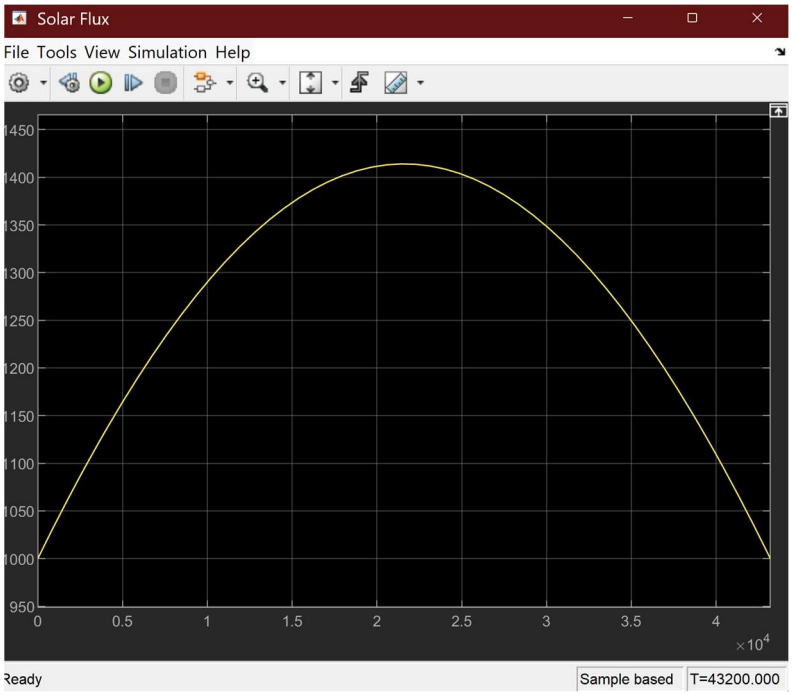


Figure 4. Solar Flux map throughout the 12-hour day

**Velocity Profile and Power Profile**

It was given in the project prompt that the electric vehicle should follow the US06 Supplemental FTP Driving Schedule supplied by the United States Environmental Protection Agency (EPA) [3]. The driving schedule, shown in graphical form in the figure below, simulates an aggressive, 596 second drive with abrupt stops and accelerations. The velocity profile for the drive is supplied by the EPA in text format.

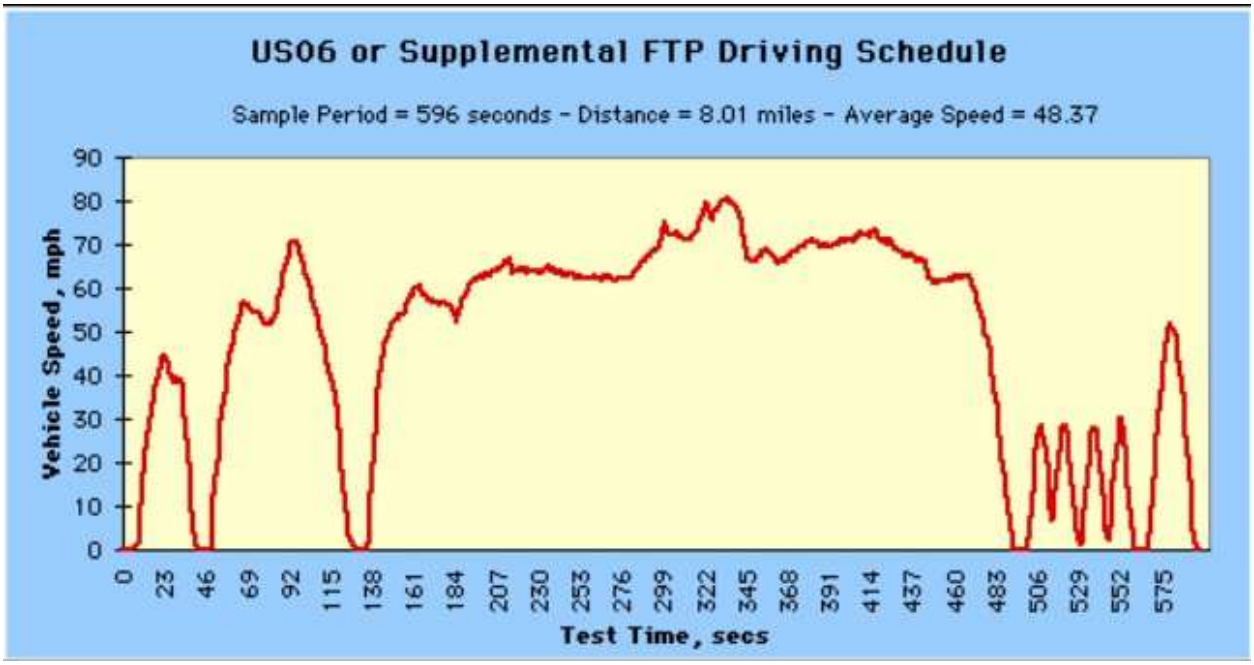


Figure 5. US EPA US06 Supplemental FTP Driving Schedule

The file was saved to excel. It was also given that the drive cycle should be repeated for 12 hours. To determine the instantaneous power throughout the drive cycle, a free body diagram of the electric vehicle was created as shown below, considering that the vehicle is in motion. For simplicity, the entire vehicle is shown as a single block. The frictional resistance overcome at the wheels is denoted by f, drag is denoted by D, lift is denoted by L, normal force from the ground is denoted by N, the weight of the car and passengers is shown pointing down, and the force required to overcome resistances and acceleration is shown by P/V. The incident angle, theta, represents the grade for the incline and decline portions of the drive.

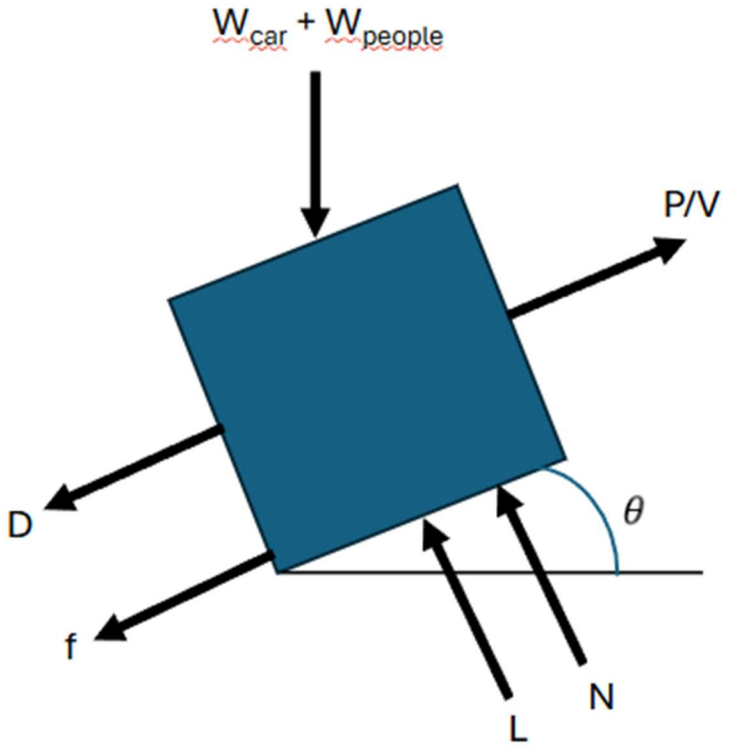


Figure 6. Free Body Diagram of Electric Vehicle

From the free body diagram, expressions were developed in order to determine the instantaneous power. The drag and lift were calculated as shown:

$$D = \frac{1}{2}\rho V^2 C_D A_{ref}$$

$$L = \frac{1}{2}\rho V^2 C_L A_{ref}$$

The instantaneous acceleration was calculated based on the instantaneous difference in velocity changes. From there, the instantaneous inertial force was calculated.

$$F_i = ma$$

The instantaneous rolling force was calculated:

$$F_r = \mu[(w_c + w_p)cos\theta - L]$$

The instantaneous total force was calculated:

$$F_t = D + F_r + F_i + (w_c + w_p)sin\theta$$

The instantaneous power was calculated:

$$P = F_t v$$

A plot of this total power is shown below:

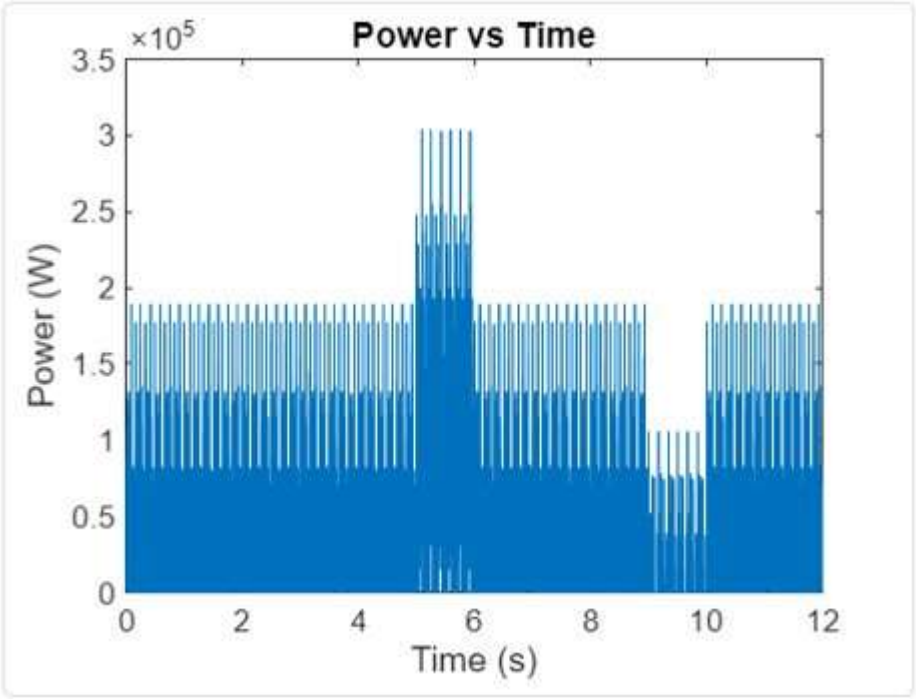


Figure 7. Instantaneous Power Plot

In order to speed up the simulation, the power was input into simscape with both positive and negative values included, and then the negative values were removed using a PS Saturation block.

**Battery System**

For this system's batteries, 3.65V 50.5Ah lithium nmc pouch battery cells were chosen [4]. These cells were chosen because they are commonly utilized in electric vehicles. Moreover, the cell specs were available.

Figure 8. Battery Cell

| Item | | Specification | Comment |
|---|---|---|---|
| Minimum Discharge Capacity | | 52.0Ah | 0.33C, 25±2℃, 2.5-4.2V |
| Minimum Discharge Energy | | 188.8Wh | 0.33C, 25±2℃, 2.5-4.2V |
| ACR | | ≤1.20mΩ | AC, 1kHz, 30%SOC |
| Nominal Voltage | | 3.63V | 1C, 2.5-4.2V |
| Weight | | 740±20g | |
| Maximum Operating Voltage (Max) | | 4.2V | |
| Minimum Operating Voltage (Min) | | 2.5V(>0℃)<br>2.0V(≤0℃) | |
| Recommended SOC Range | | 10%-90%SOC | |
| Standard Charging Current | | 17.3A | 1/3C |
| Standard Discharging Current | | 17.3A | 1/3C |
| Cycle Life | 0.33C/0.33C @25℃ | 3000 cycles | Capacity retention: ≥80% |
| | 0.33C/0.33C @45℃ | 1000 cycles | Capacity retention: ≥80% |
| Cell Dimensions | Length | 301.5±1.0mm | |
| | Width | 99.7±2.0mm | |
| | Thickness | 11.6±0.2mm | 30%SOC, 800±300N, ≤10sec |
| Operation Temperature | Charge Temperature | -20~55℃ | |
| | Discharge Temperature | -30~55℃ | |
| Storage Temperature | 1 year | 0~25℃ | At Shipping SOC |
| | 3 months | 0~45℃ | |
| | 1 month | 0~60℃ | |

Figure 9. Battery Cell Specifications

These cells were added until the resulting capacity matched the capacity required based on the power draw of the system.

The total power draw of the system at the wheels is 430 kWh as calculated by the following:

$$P_{kWh} = P_{avg} \times 12hrs \div 1000$$

In simscape, each cell was discretized into two parts for conduction. Each cell was conductively connected to each other using a thermal interface material. The cells were connected together to create 8 individual battery packs as shown below [5].

Figure 10. Battery Layout in Electric Vehicle

Each battery is surrounded by a water jacket. The water jacket includes a 50% water/ethylene glycol mixture.

The overall battery system in simscape is modelled as follows with 8 batteries total.

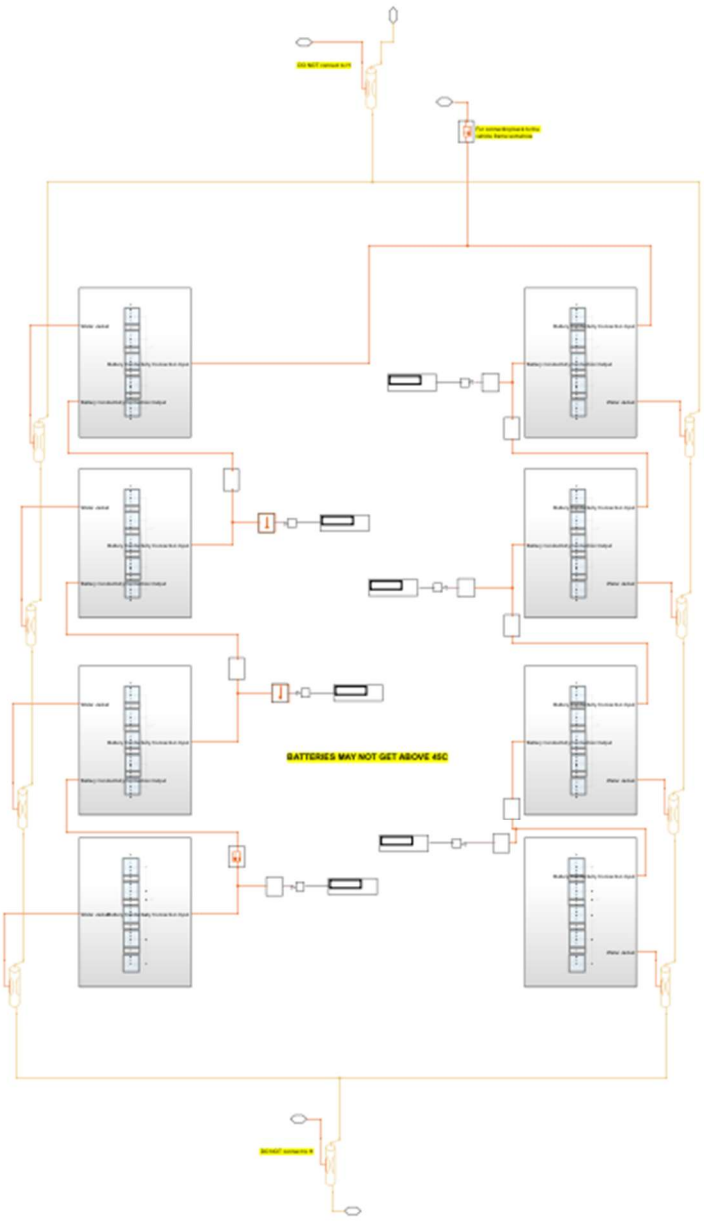


Figure 11. Simscape Battery Layout

Each battery is a stack up of 5 lithium NMC cells, with the water jacket externally covering the stack up. A thermal interface material was chosen to be 50-3186 NC due to its high thermal conductivity [6]. The battery specific heat capacity was chosen to be the generic heat capacity for a lithium NMC cell [7].

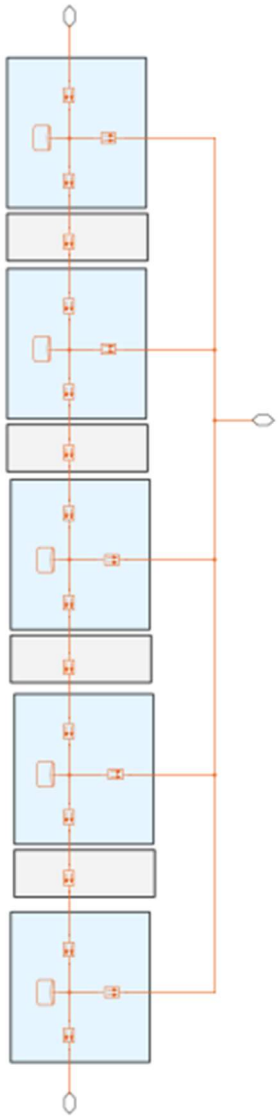

Figure 12. Simscape Battery Cell Stack Up

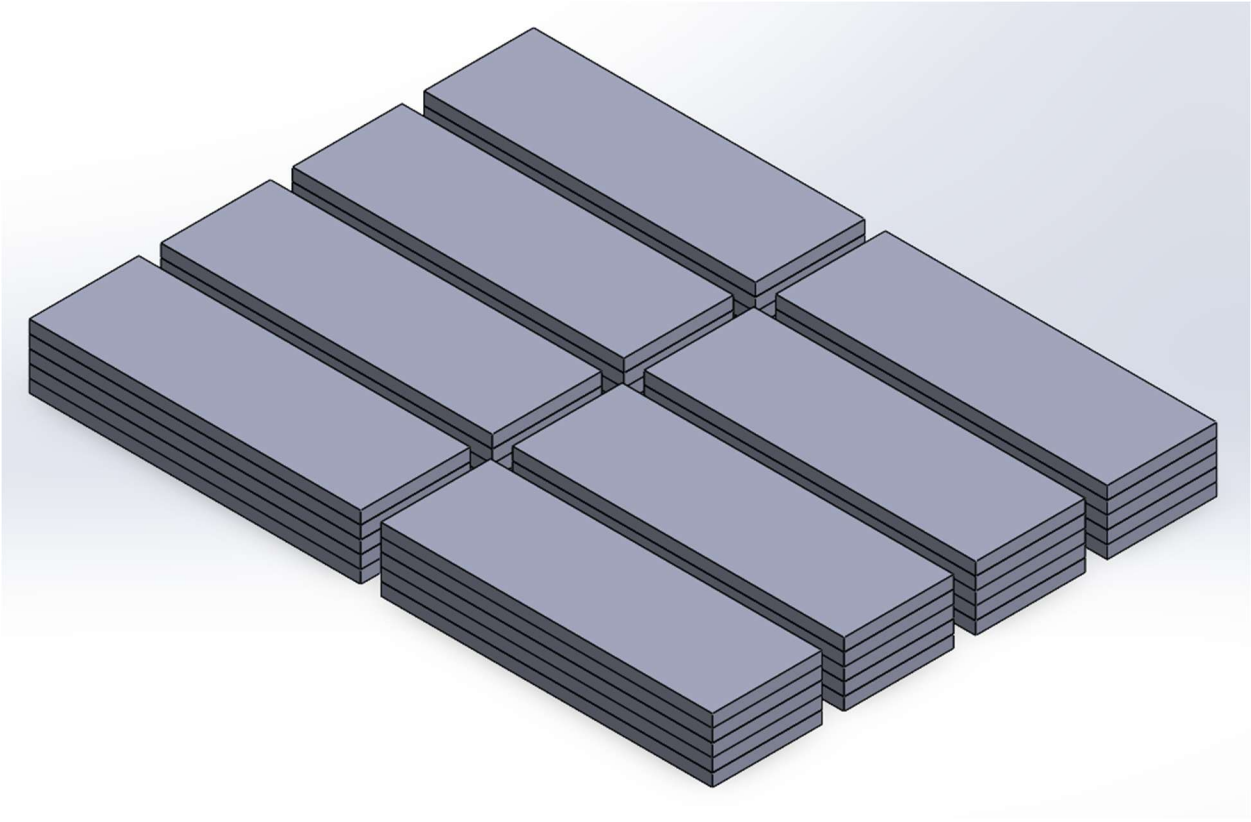

Figure 13. 3D Model of Battery Layout

**Cabin Interior & HVAC**

To size the cabin interior of the EV, a few assumptions were made. The cabin interior of the car is roughly based on the ratios of a 2025 Regular length, Low Roof Ford Transit. The air volume within the cabin is approximately the same ratio as the specifications of the Ford Transit and the window sizes are approximated as 40” x 40” for the two side windows and 40” x 55” for the front windshield. The side windows are vertical, and the front windshield is angled at 60° from horizontal. The windows are modeled as completely transparent to maximize the solar load on the cabin air and size the HVAC for the worst-case scenario. The car is assumed to be airtight and insulated, so that the only significant external heat transfer occurs via the windows. The cabin air is assumed to be isothermal throughout the interior and receives forced convection from the HVAC and natural convection from the windows.

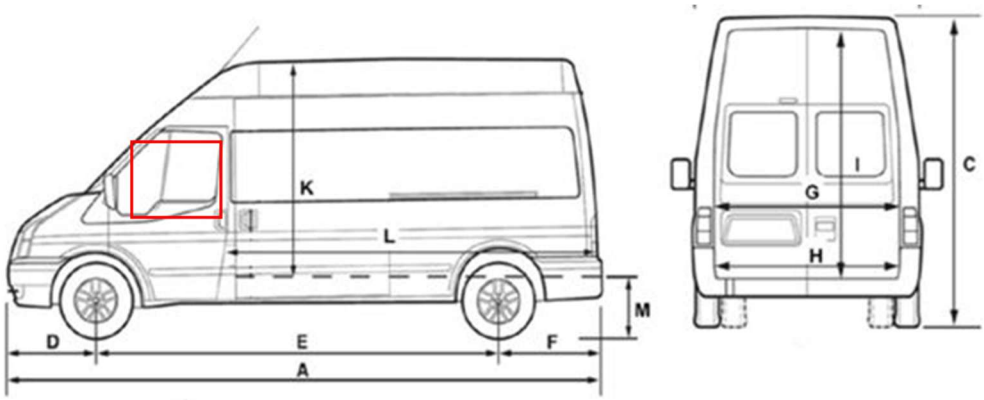


Figure 14. Window Ratio of 2025 Ford Transit

The thickness of the glass was modeled as a standard thickness of 0.25 in and the thermal and physical properties of each window are listed in Table 1 [8], [9].

Table 1. Physical and Thermal Properties of Windows

| | Side Windows | Front Window |
|---|---|---|
| Density (kg/m$^3$) | 2500 | 2500 |
| Surface Area (in$^2$) | 1600 | 2200 |
| Thickness (in) | 0.25 | 0.25 |
| Thermal Conductivity (W/m/K) | 1.05 | 1.05 |
| Angle (°) | 90 | 60 |

To design an HVAC that keeps the interior air at 70 °F, it is imperative to first model the heat loads acting upon the cabin air. Starting at the windows, the variable velocity of the car generates forced external convection from the exterior temperature to the outer surface of the window. The forced and free convections were modeled for each window using a vertical plate correlation for the side windows and an angled plate correlation for the front windshield. Figure 15 shows the topology of the external convection and window subsystems.

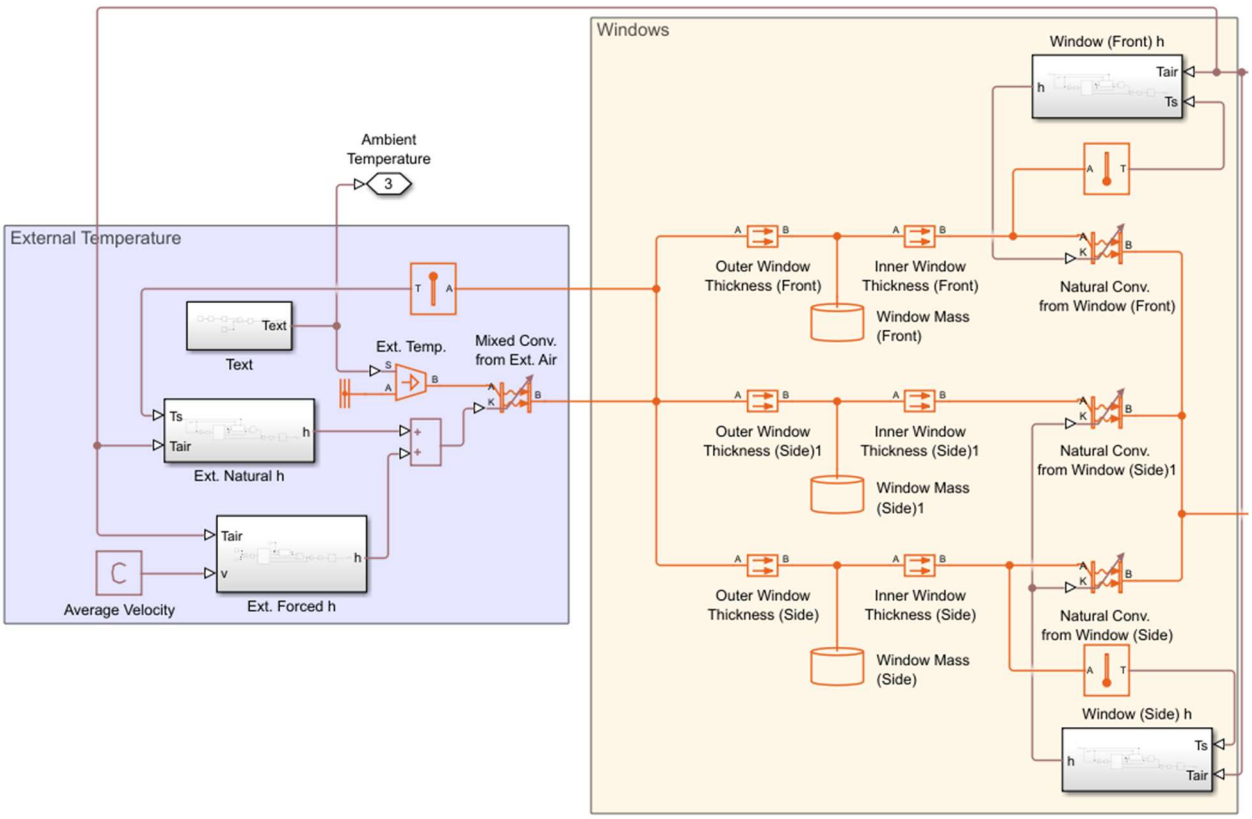


Figure 15. Topology of External Convection and Windows

The velocity profile of the car was averaged to a constant 48 mph to cut simulation time. Using the exact velocity profile yielded no visible difference in effect on cabin air temperature or required work in, as shown in Figures 16 and 17.

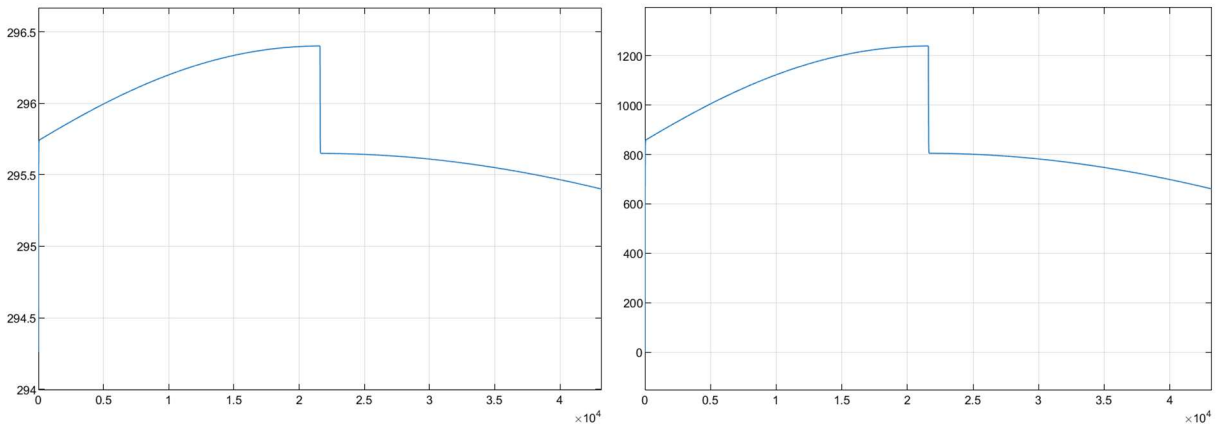


Figure 16. Cabin Air Temperature (Left) and Required Work In (Right) using Exact Velocity

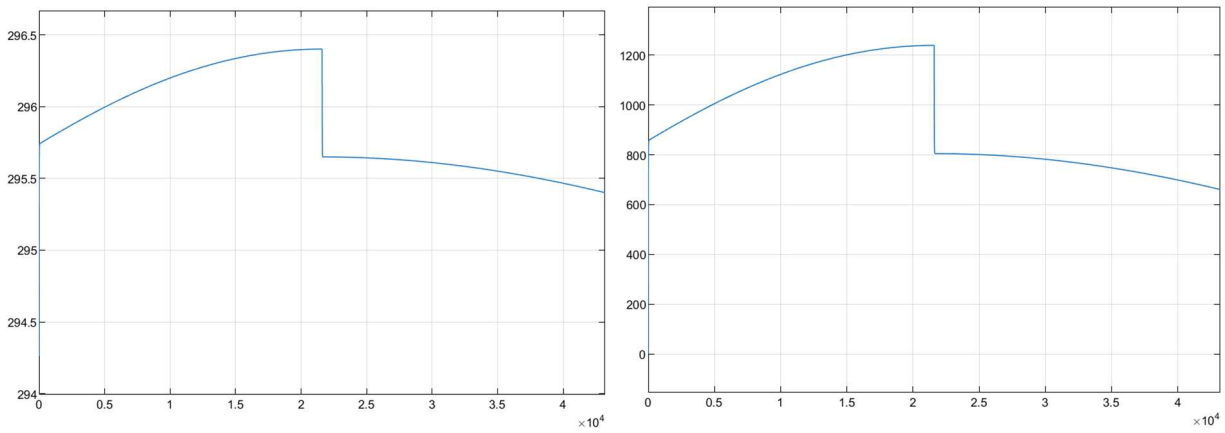


Figure 17. Cabin Air Temperature (Left) and Required Work In (Right) using Averaged Velocity

Next, the internal loads can be modeled. A major internal load here is the solar load. The solar load is composed of direct and diffuse parts, where all the windows experience a diffuse solar load as the surroundings reflect light from the sun into the car. Only the front windshield experiences direct solar load. This is because the side windows never view the sun at any point in the simulation, as they are vertical and the sun is assumed to travel directly overhead of the car. The direct solar load that the front windshield experiences is dependent on the sun's zenith angle, as the front windshield is in line with the path of the sun. The reflectance of the surroundings is taken to be 0.20, as averaged from the values for concrete and wood [10]. Figure 18 shows the solar load model.

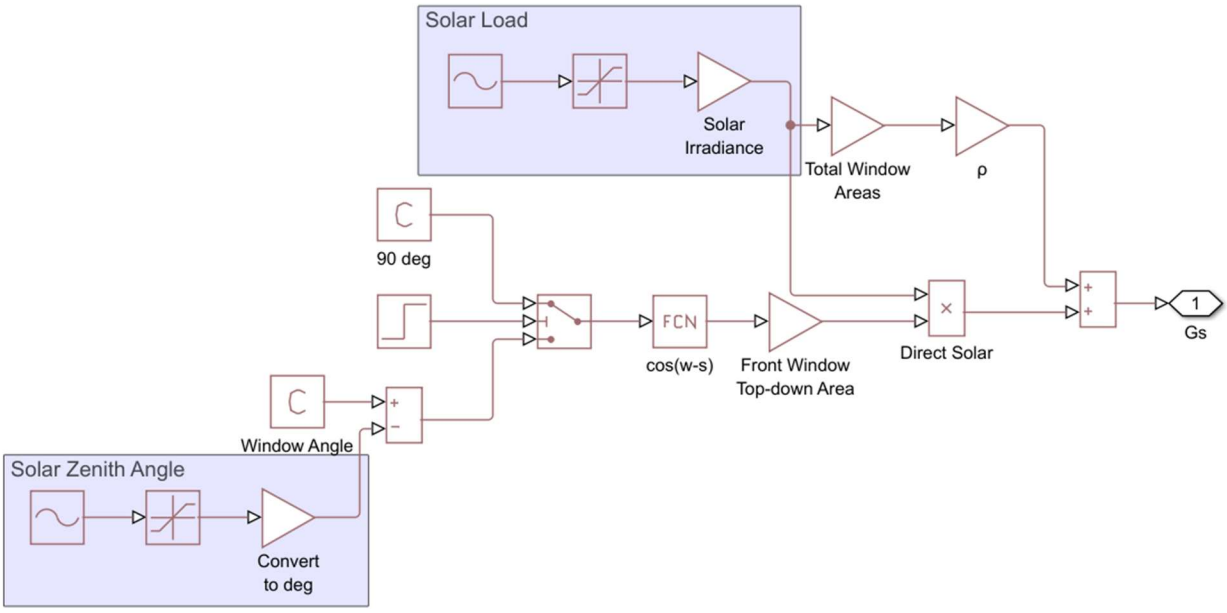


Figure 18. Solar Load Model

The solar load is directly fed into the cabin air, as the windows are completely transparent. Another load directly fed into the cabin is the passenger loads. Given the requirement of a 6-passenger vehicle and the metabolic rate of one person is 104 W, the total passenger heat load is 624 W [11]. The passengers are treated simply as loads as their mass and convection will have a negligible effect on the cabin air temperature, which is to be kept at 70 °F. The cabin air mass is found by taking 1/3 the volume of the cabin, like the ratios of a Ford Transit, which results in an air volume of 7.81 m^3 and a mass of 9.40 kg [12].

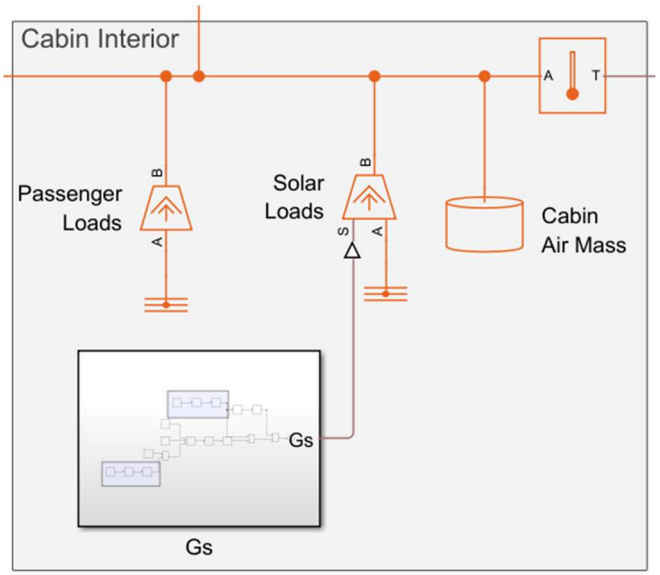


Figure 19. Topology of Cabin Interior

The final load is from the HVAC system, which is modeled as forced convection from a 70 °F temperature source to the cabin air mass. The forced convection coefficient is taken from the flat plate correlation where the plate's length is equal to the length of the car and the air velocity is a constant 100 ft/s [13]. The heat flow rate between the HVAC source and the cabin air is measured and modeled as a dissipation to the coolant loop. The same physical signal is divided by the coefficient of performance of 2, the product of which represents the transient required work in from the battery [14]. Figure 20 shows the topology of the HVAC system.

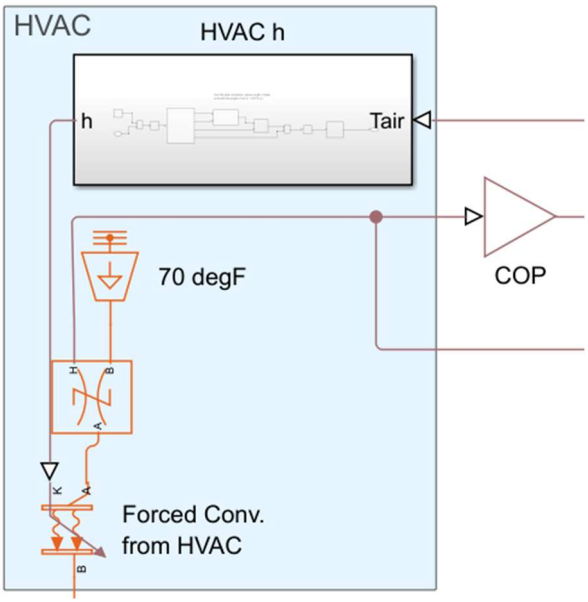


Figure 20. Topology of HVAC

## Radiator

The main function of the radiator of the car is to expel all the heat the coolant is currently carrying back into the atmosphere before the coolant loops back into the system. The start of this design was on the gas side. First was setting the proper gas properties, and this was done with the assistance of CoolProps to calculate all the properties going off of the temperature and pressure vector, as seen below [15].

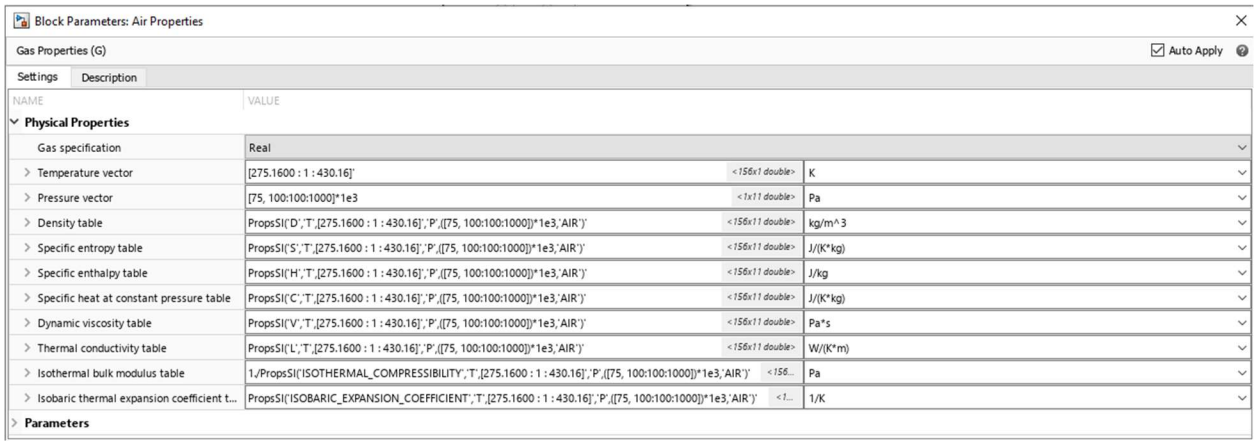


Figure 21: Air Properties

Next was the determination of the temperature of the ambient air. Due to the environmental loading conditions, the ambient air is steadily changing throughout the day, which is an important factor as the radiator being the only way to expel heat, and increasing ambient air

temperature leads to lower heat dissipation into the air as the difference in temperature decreases between the air and the coolant.

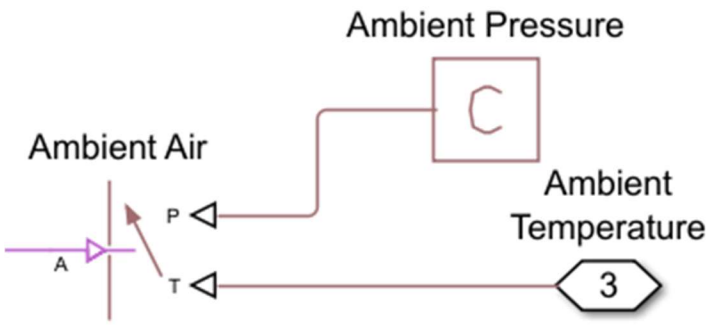


Figure 22: Ambient Air Reservoir

Since the air can be taken as an infinite source throughout the drive, a controlled reservoir was used, with an ambient pressure of 101325 Pa, and with the varying temperature. The ambient temperature connect port is connected to the HVAC subsystem, directly to the external temperature that is being calculated.

To make ease with iterations, constant flow rate sources were used in the model to have a consistent flow rate running throughout the model as it would be possible to mess with the flowrate directly instead of converting RPM to the flowrate of a pump or fan. The pumps and radiator fan were to be added in after it was proven the model can run without the coolants overheating at a given flowrate.

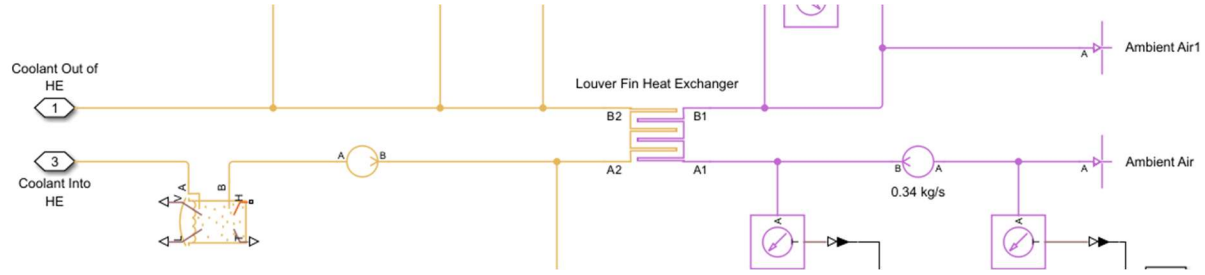


Figure 23: Preliminary Set-Up

For the flow rate of the air, our starting point was a mass flowrate of 0.34 kg/s, as previous homework as well as the thermal design handbook have that mass flow rate listed throughout [16]. Higher flowrates were attempted but were unsuccessful as the air was traveling through the heat exchanger too fast where it was not absorbing significant heat. To size a radiator, we first had to convert the mass flowrate to volumetric flow rate, which was achieved by finding the density of air at our average temperature, and dividing the mass flow rate to obtain

our goal volumetric flow rate, which was at 0.2886 m^3/s. From there, a radiator fan was found for reference that could operate within that volumetric flow rate, and in the end an SPAL fan was chosen.

blowing / *soffiante*

| Airflow *Portata* m³/h | Current input *Corrente assorbita* A | Airflow *Portata* CFM | **Static pressure *Pressione statica*** $inH_2O$ |
|---|---|---|---|
| 2190 | 12,6 | 1292 | 0 |
| 1910 | 13,1 | 1127 | 0,2 |
| 1590 | 13,4 | 938 | 0,4 |
| 1460 | 14,3 | 861 | 0,5 |
| 1200 | 13,7 | 708 | 0,6 |
| 820 | 13,9 | 484 | 0,7 |
| 470 | 13,2 | 277 | 0,8 |
| 320 | 13,4 | 189 | 0,9 |
| 120 | 13,6 | 71 | 1 |
| 0 | 14,3 | 0 | 1,2 |

Figure 24: Fan Specifications [17]

For the heat exchanger between the coolant and the ambient air, it was asked to be an air to liquid louver-fin type heat exchanger. To get the initial design parameters, the thermal design book once again was of assistance, specifically chapter 4.9, a section dedicated entirely to louver-fin heat exchangers [16].

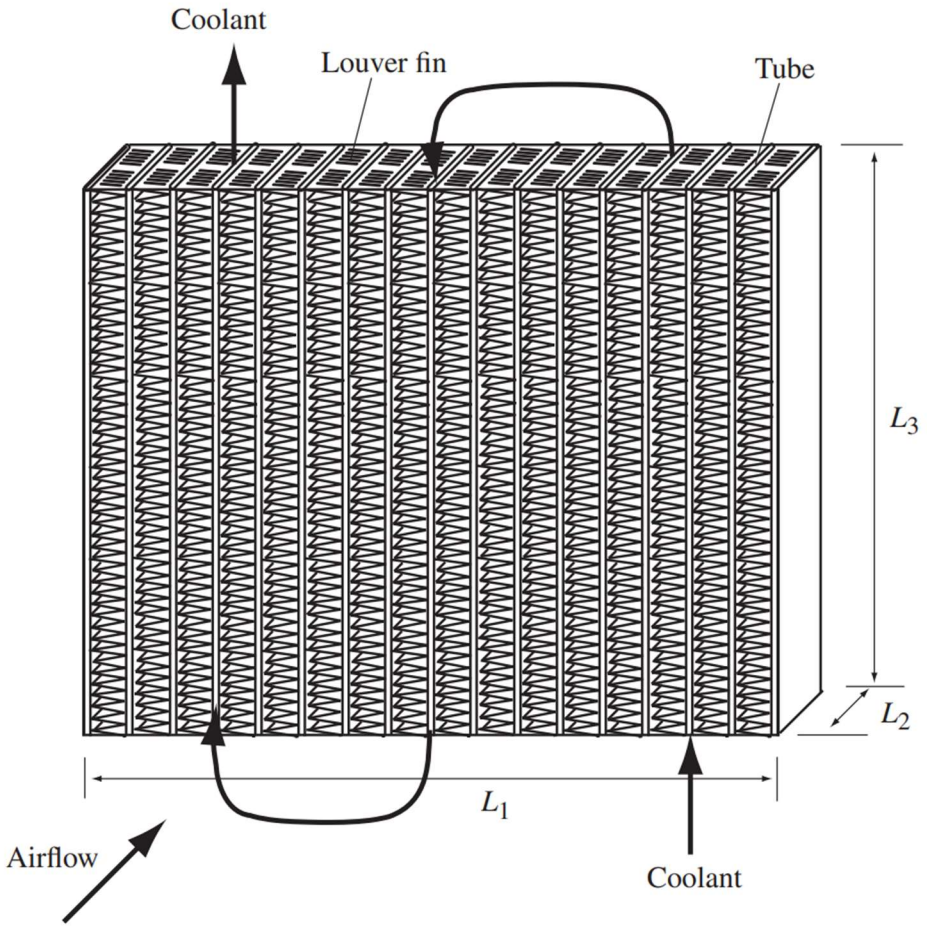


Figure 25: Louver-Fin Heat Exchanger [16]

Using the equations from the textbook as well as the correlations for the louver fin geometry, a preliminary design was optimized to obtain the starting dimensions and geometry of the heat exchanger. In the end, we obtained the following parameters for the louver-fin heat exchanger as shown below.

| Gas 1 | | |
|---|---|---|
| Minimum free-flow area | 0.0728 | m^2 |
| Hydraulic diameter for pressure loss | 1.3832 | mm |
| Gas volume | 0.01 | m^3 |
| Laminar flow upper Reynolds number li... | 2000 | |
| Turbulent flow lower Reynolds number l... | 4000 | |
| Pressure loss model | Correlation for flow inside tubes | |
| Length of flow path from inlet to outlet | 15.0000 | mm |
| Aggregate equivalent length of local re... | 1 | m |
| Internal surface absolute roughness | eps | mm |
| Laminar friction constant for Darcy fricti... | 64 | |
| Heat transfer coefficient model | Tabulated data - Colburn factor vs. Reynolds number | |
| Heat transfer surface area | 3.1572 | m^2 |
| Length of flow path for heat transfer | 15.0000 | mm |
| Reynolds number vector for Colburn fac... | [1:1:4000,5000:10^4:10^8] | |
| Colburn factor vector | 0.4448*([1:1:4000,5000:10^4:10^8]).^(-0.49) | |
| Fouling factor | 0.352e-3 | K*m^2/W |
| Threshold mass flow rate for flow reversal | 1e-4 | kg/s |
| Minimum gas-wall heat transfer coeffici... | 5 | W/(K*m^2) |

Figure 26: Air Side Parameters

For dimensions, the radiator came out to a width of 2.3 feet, 0.5374 ft in height, and a depth of only 15 mm, making it fit perfectly into the Ford transit model.

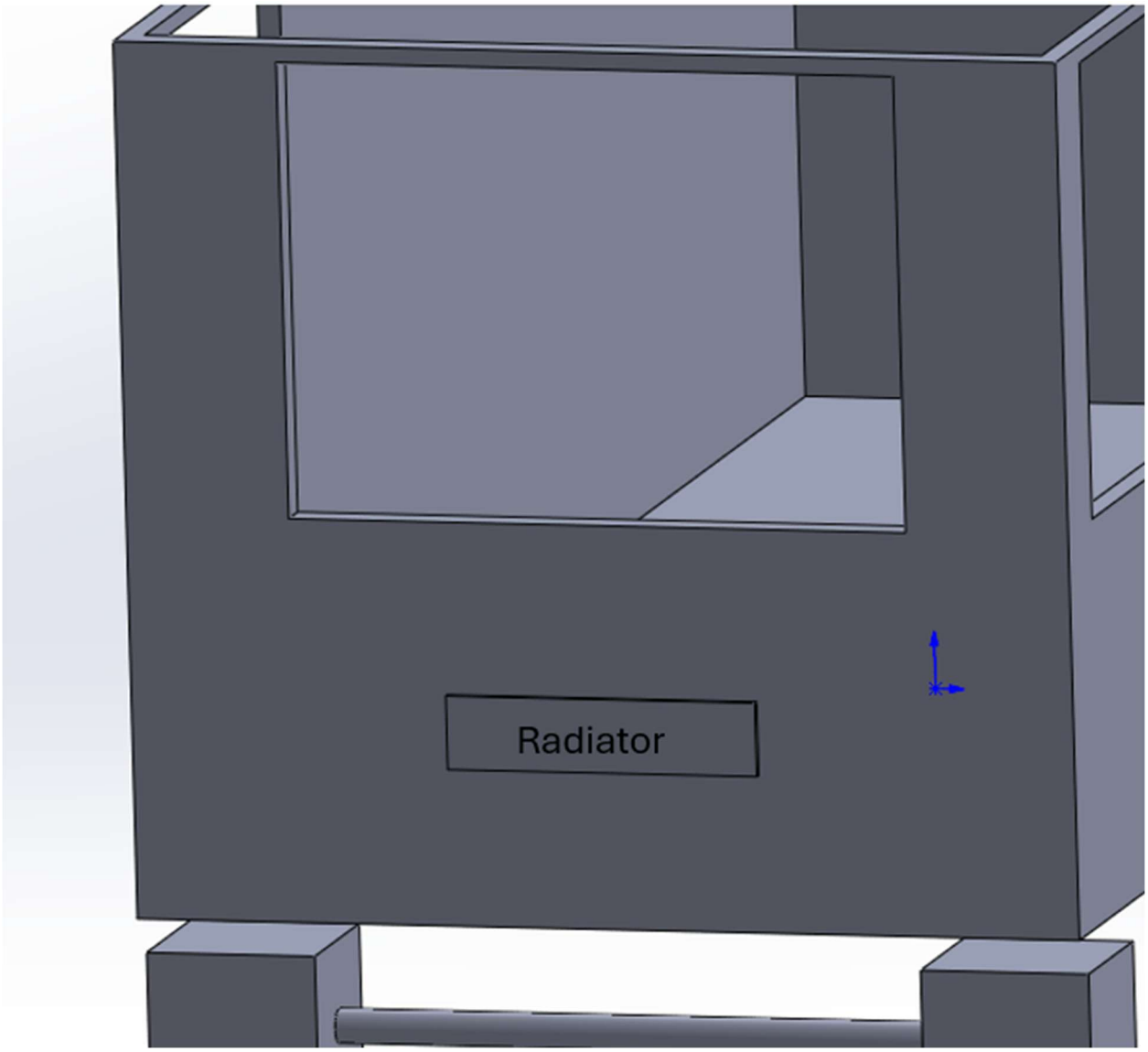


Figure 27: Radiator on Ford Transit

| Thermal Liquid 2 | | |
|---|---|---|
| Minimum free-flow area | 2.4887e-04 | m^2 |
| Hydraulic diameter for pressure loss | 0.0025 | ft |
| Liquid volume | 0.01 | m^3 |
| Laminar flow upper Reynolds number li... | 2000 | |
| Turbulent flow lower Reynolds number l... | 4000 | |
| Pressure loss model | Correlation for flow inside tubes | |
| Length of flow path from inlet to outlet | 0.5374 | ft |
| Aggregate equivalent length of local re... | 75.1867 | mm |
| Internal surface absolute roughness | eps | um |
| Laminar friction constant for Darcy fricti... | 64 | |
| Heat transfer coefficient model | Correlation for flow inside tubes | |
| Heat transfer surface area | 0.2176 | m^2 |
| Length of flow path for heat transfer | 239.7125 | mm |
| Nusselt number for laminar flow heat tr... | 7.541 | |
| Fouling factor | 0.176e-3 | K*m^2/W |
| Minimum liquid-wall heat transfer coeff... | 5 | W/(K*m^2) |
| Effects and Initial Conditions | | |

Figure 28: Coolant Side Parameters

For the coolant side, an Ebara EVMS (L)1 10/0.55* pump was selected as it was found that the coolant needed to flow at a rate of about 20 L/min in order to avoid overheating before it could arrive at the louver fin heat exchanger. It was found when sizing the pump that a speed of 600 RPM hovered close enough to the 20 L/min speed needed for the coolant loop.

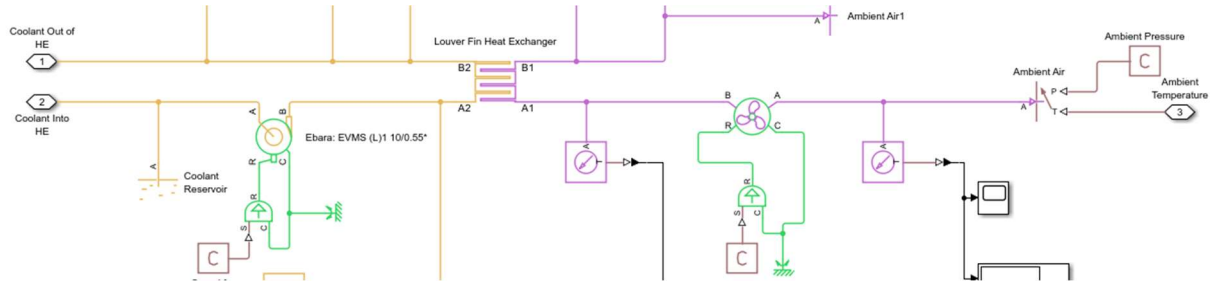


Figure 29: Radiator System

## Inverter Cold Plate

The inverter is represented with 5 IGBTs that are connected to a PCB. There are four inverters total, per motor, that power is equally distributed to. Due to the efficiency of the inverter the junction temperature of the IGBTs must be managed by a cold plate heat exchanger and kept under 125degC. Upon research of PCBs a model from Infineon with a surface area of 21.5mm by 16.3mm will be applied to the thermal interface material [18]. The IGBTs have a resistance of 0.1 K/W, as given in the problem statement. The PCB resistance is assumed to be

infinitely large so that the heat flow path from the PCB is going directly to the designed heat sink. Although this isn't a realistic condition as there would definitely be heat dissipated into the PCB, this accounts for a worst-case condition and any other heat flow paths would further assist in the cooling of the IBGTs. There is a copper cold plate attached to the PCBs with an area of 0.0108 m² and thickness of 5 mm, which also has a very low resistance of 0.00115 K/W given that copper has a low thermal conductivity of 401 W/m/K [16]. The thermal interface material is Artic Silver 5 thermal paste with a thermal conductivity of 8.9 W/m/K and a bond line thickness of 1 mil [19]. The overall series resistance of the IGBT, thermal interface materials, and the copper plate is 0.102 K/W, thus allowing adequate heat to be dissipated into the fluid within the cold plate.

The Simscape topology of the inverter system is set up with a controlled heat flow block going into the IGBT junction to case resistance. Following that are two conductive resistance blocks that represent the thermal interface material and the copper plate, respectively. Connected to the other end of the thermal plate is a Thermal Liquid Pipe block which represents the channel within the cold plate. There are 5 identical configurations of this in parallel to model the heat flow paths from the IGBTs to the fluid (Figure 30). This means that the fluid channel was discretized into 5 segments.

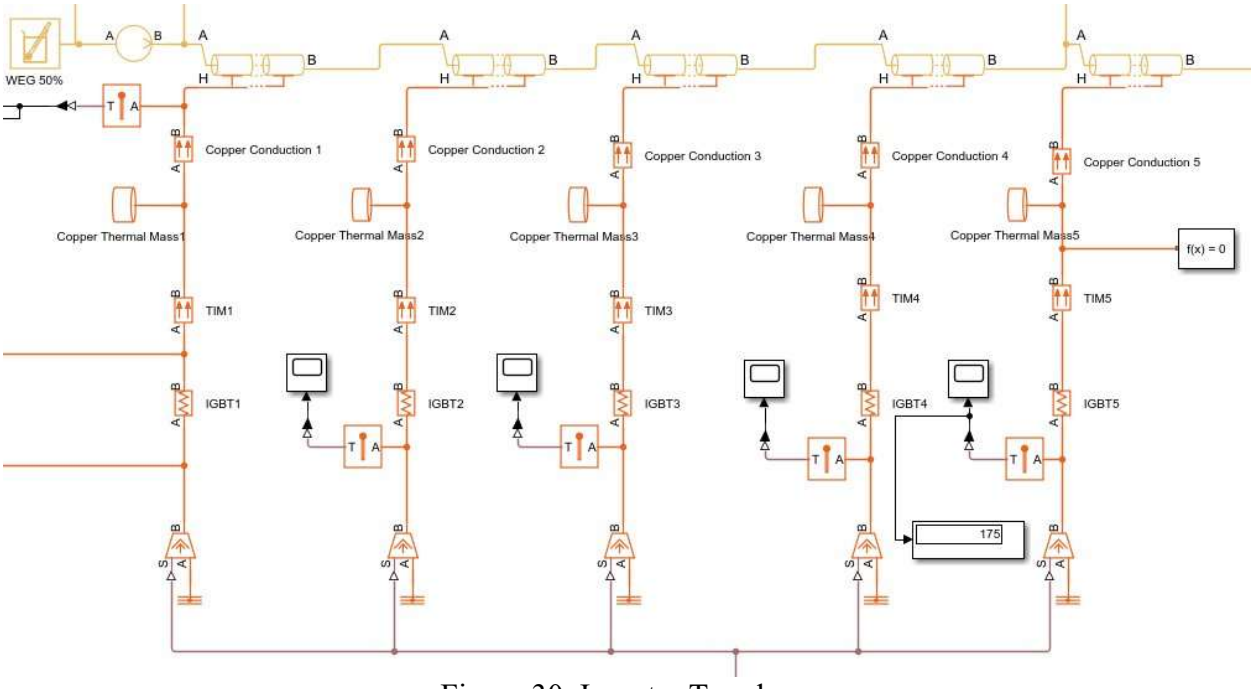


Figure 30. Inverter Topology

The cooling fluid that passes through the cool plate is 50% Water Ethylene Glycol that must have an inlet temperature at a maximum of 50 ˚C, which was a given requirement. The flow rate of the fluid is about 20 L/min and the channel has a width of 350 mm and a height of 4 mm. The overall length of combined 5 segments is 750 mm.

**Engine-Gearbox Subsystem**

For the motor units of the electric vehicle, all motors were modeled the same, as shown in the figure below.

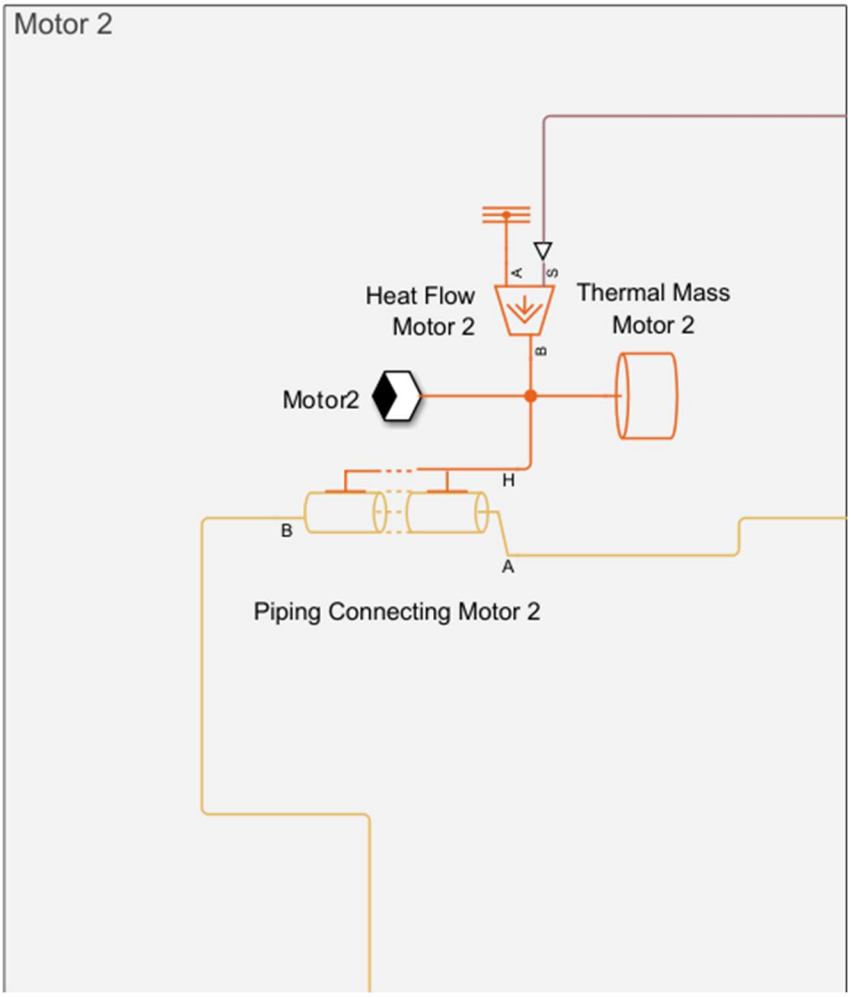


Figure 31: Motor Thermal Layout

As can be seen, there is a controlled heat dissipation that is connected to a thermal mass and then to a pipe. The heat dissipation is controlled by the drive cycle that was mentioned earlier.

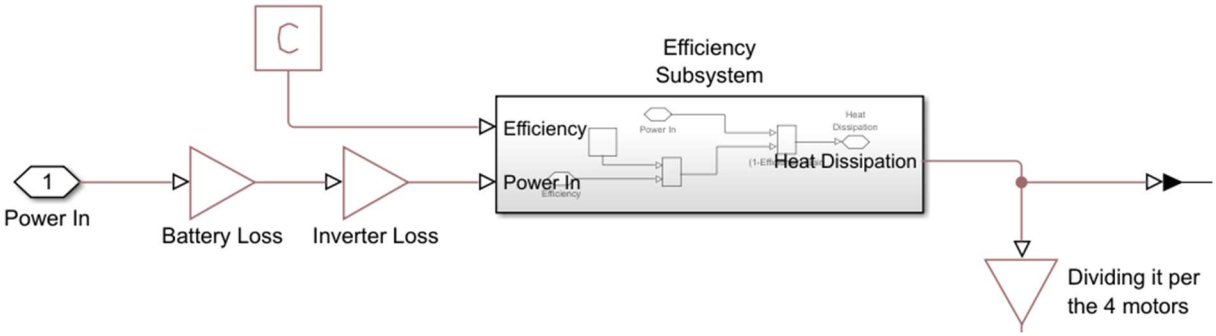


Figure 32: Power Breakdown

We have the total power that is being released from the battery into the motor subsystem, where it first travels through two gain blocks. Each gain block is labeled with their effect, which is the power lost due to the efficiencies of the other systems before it has reached the motor. For example, the battery has an efficiency of 90%, therefore before it enters the inverter system, it has lost 10% of the power to heat, so this is reflected in the motor subsystem as a gain of 0.9.

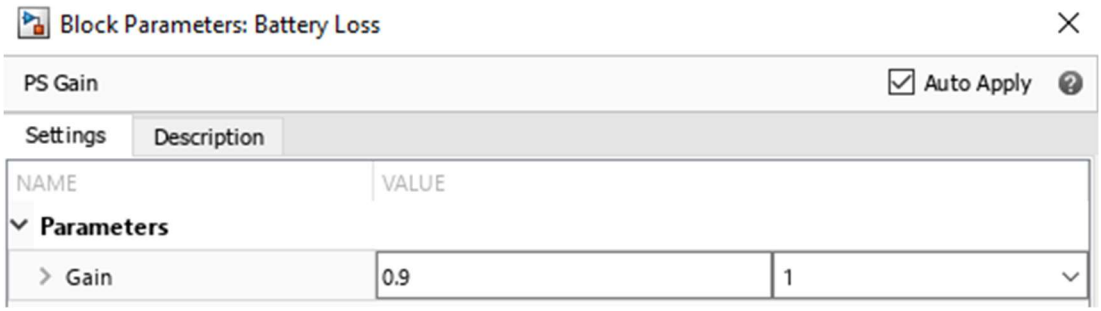


Figure 33: Battery Loss Gain

On the top of Figure 32, a constant block can be seen, which is the efficiency of the current subsystem, in this case being the motors. Since the motors have an efficiency of 80%, 0.8 was the number put into the constant block. From there, the true power hitting the motor and the motor efficiency block enter the efficiency subsystem. Within this subsystem is a very simple calculation but was made into a subsystem for ease of implementation across all systems in this model.

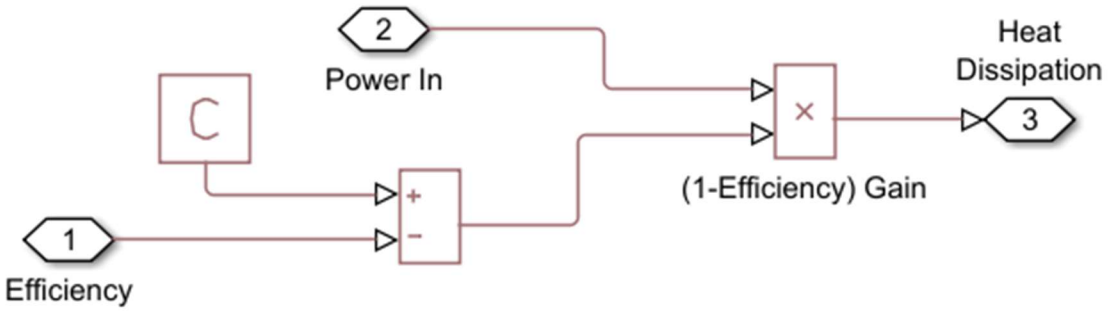


Figure 34: Efficiency Subsystem

As can be seen, it simply takes the current efficiency, and subtracts it from 1, giving us the percentage of power that is to be converted into heat dissipation. Once that percentage is calculated, it is multiplied by the total power entering the system to get the heat dissipation that is to be expected. From there, one more gain is applied to the heat dissipation signal before it enters the controlled heat flow, as seen in the bottom corner of Figure 32. The purpose of this is to distribute the heat flow evenly among the four motors. To split it into four, a simple gain of 0.25 was inputted.

Getting back into the motor unit, the next portion is the thermal mass. It was found that a Tesla model 3 motor unit weighs around 80 kg [20]. Since it is known that the motor is not 100% solid, a 40% reduction was put on thermal mass to get a total of 48 kg. As for the material, it was chosen to be made of steel as that is the most common material for gearboxes.

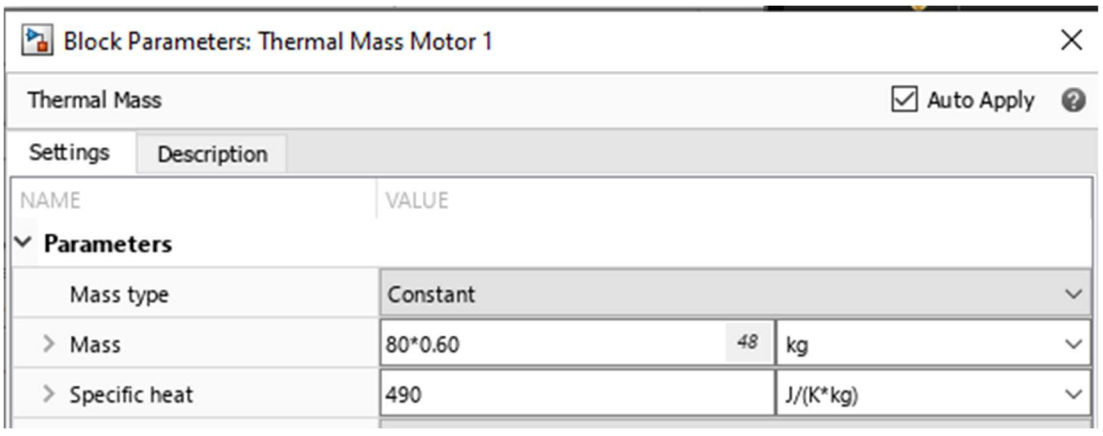


Figure 35: Thermal Mass for Motor / Gearbox

The next connection leads into the thermal liquid pipe to transfer the heat dissipation away from the motors and towards the oil.

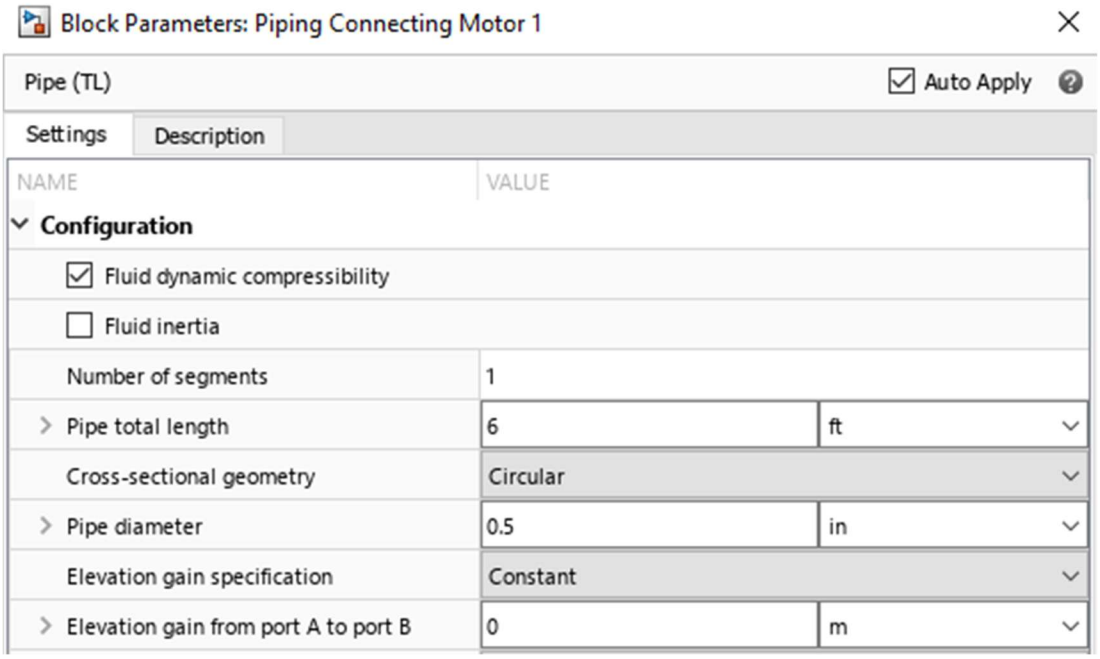


Figure 36: Motor Piping Parameters

For the piping connected directly to the motors, it was assumed that the pipe was to loop back and forth multiple times to extend the amount of time the oil would stay in thermal contact with the heat dissipation. For the pipe diameter, both for the direct connections to the motors as well as the regular pipes connecting the full loop, it was found that the average oil pipe size was 0.75 in [21]. For the distance between the vehicle's wheelbase, research concluded that the distance was 130 inches [12].

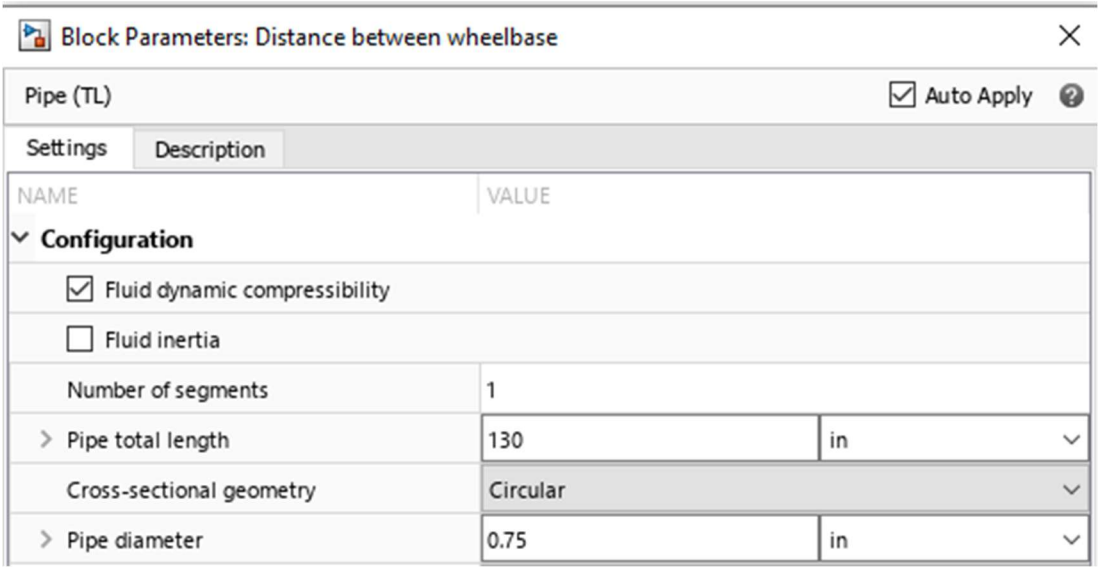


Figure 37: Wheelbase Distance Pipe

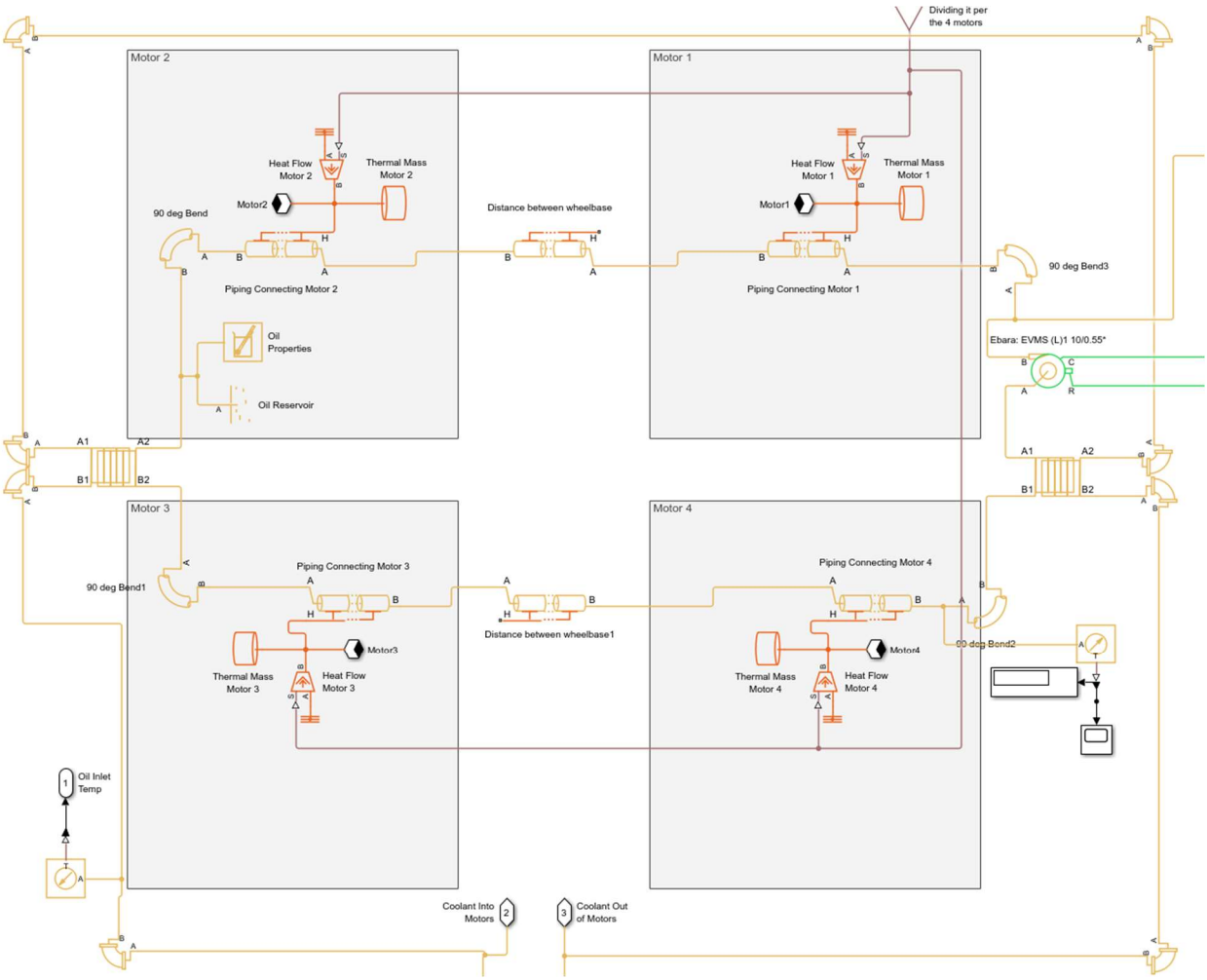


Figure 38: Total Motor System

For the oil loop, the design asked for SAE 5W-30 to be used. Using Coolprops once again, the closest to engine oil was DowQ transmission oil, so with the assistance of the CoolProps callouts, we defined the oil parameters [15].

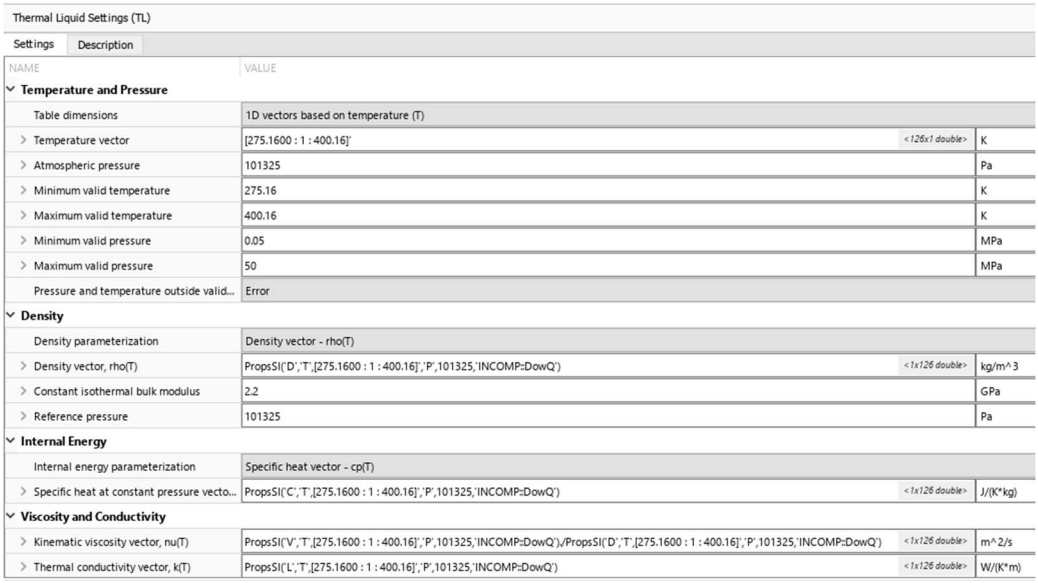


Figure 39: Oil Parameters

The oil then loops between the four motors within its own pipe network, expelling heat by interacting with two plate heat exchangers.

For the plate heat exchangers, once again the thermal design handbook was used for the initial sizing and parameters [16].

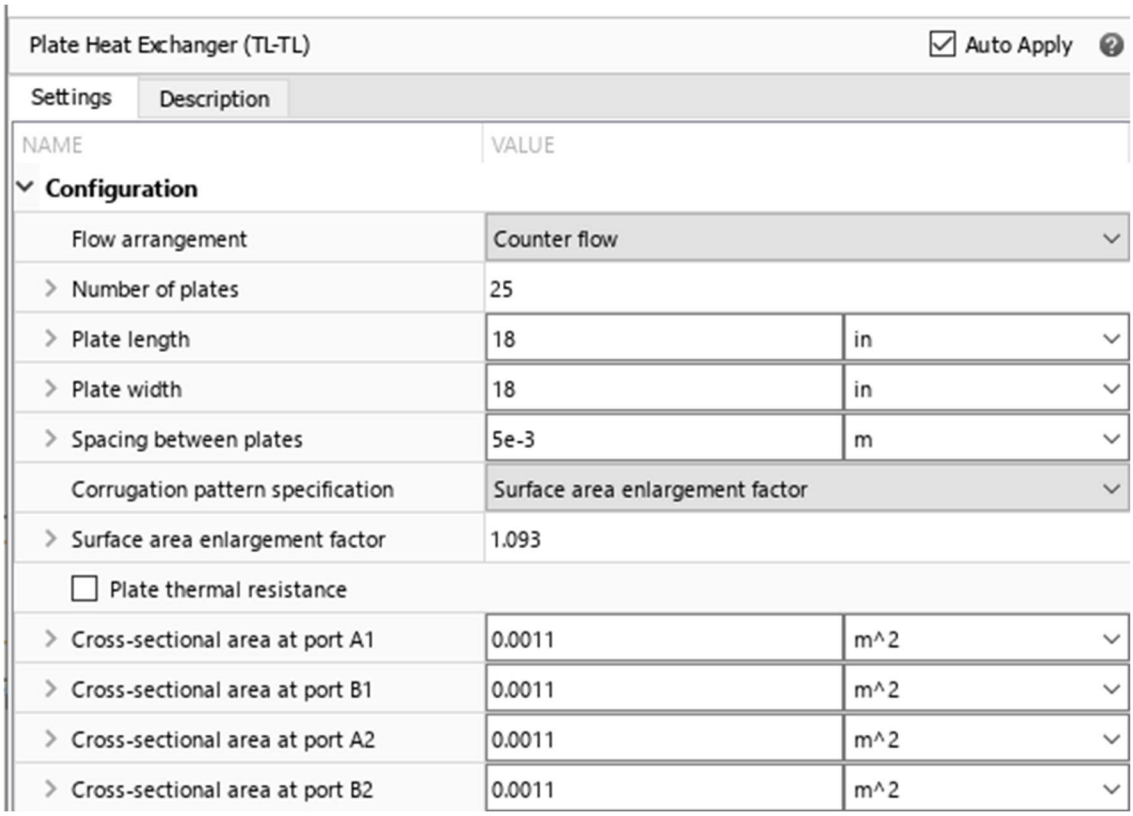


Figure 40: Plate Heat Exchanger Parameters

These two plate heat exchangers are connected to the system coolant loop that travels within the vehicle. The coolant enters the motor system and interacts with each heat exchanger once before exiting the motor system and heading into the radiator.

The same pump being used for the coolant loop was chosen for the oil loop as the same flowrate of 20 L/min was needed to cool the motors.

**Thermal Plumbing**

The thermal plumbing of the system is the most important aspect thermally, as it is the only way the vehicle is able to expel heat. The thermal plumbing starts within the radiator system as that is the start and end of the coolant loop, where it comes into contact with the louver fin heat exchanger and expels the heat into the ambient air. From there, the coolant travels within its own loop. Because of the different design criteria set, such as maximum motor temperature of 100°C or maximum oil temperature of 90°C before the motor subsystem, the pathway of the coolant had to be specific. It would first travel through the HVAC system to absorb the heat load is was expelling, as it had the lowest temperature of 70°F. From there, it moves onto the battery system, which needs the batteries to be at an operating temperature of less than 45°C. Then the last two system the coolant travels through are the inverters and then motors as that was the

design criteria, as well as the two hottest temperatures the coolant would experience, before it wraps back around to the radiator.

For the HVAC section, the amount of heat that is being dissipated out of the cabin is obtained as a physical signal, which is connected to a controlled heat flow block that dissipates the heat into a thermal liquid pipe carrying the coolant.

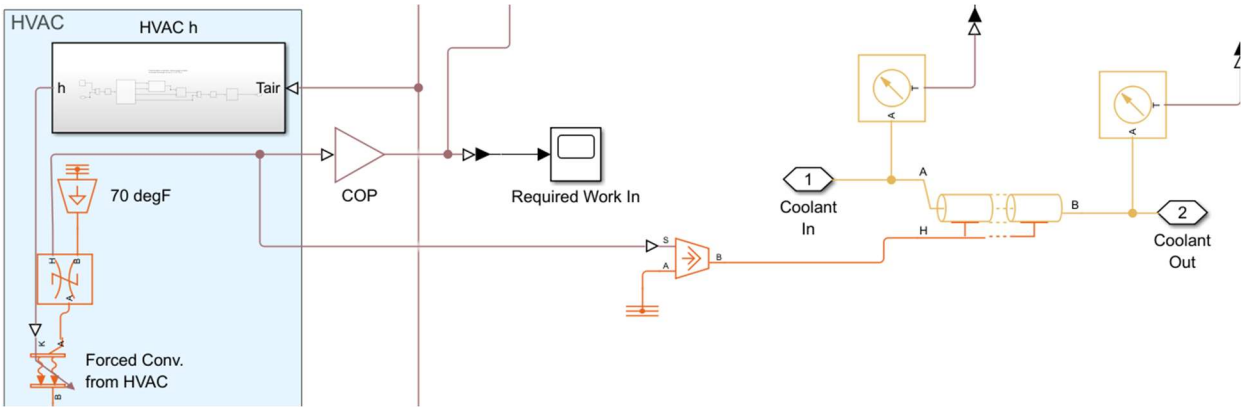


Figure 41: HVAC Coolant Connection

From there, the coolant is split into two parallel pipes to each be connected to 4 batteries before converging into a single pipe again and heading into the inverters, where it splits in four to cover them in parallel.

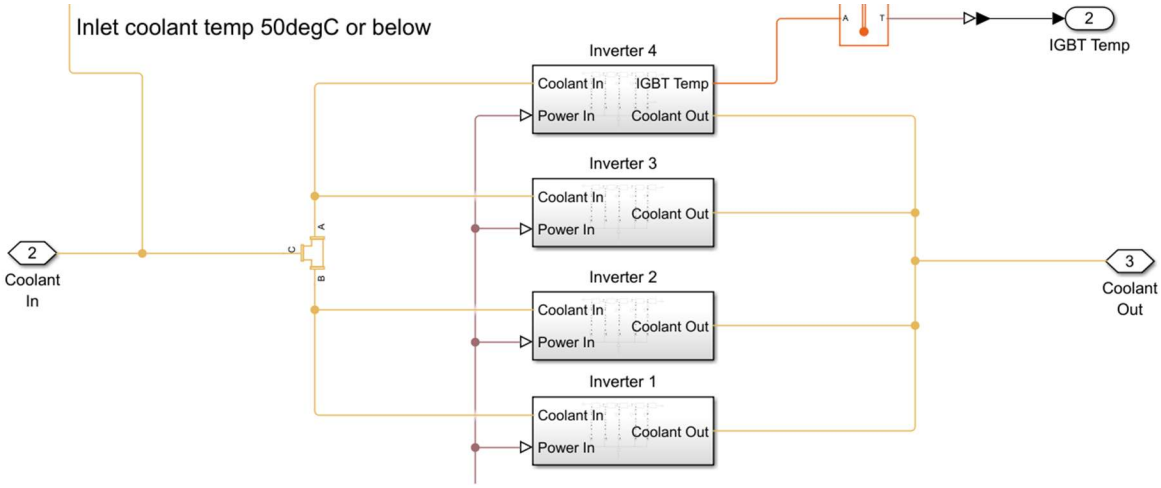


Figure 42: Inverter Coolant Connection

The last connection is to the plate heat exchangers of the motor subsystem where the transmission oil expels its heat to the coolant before the coolant heads to the radiator.

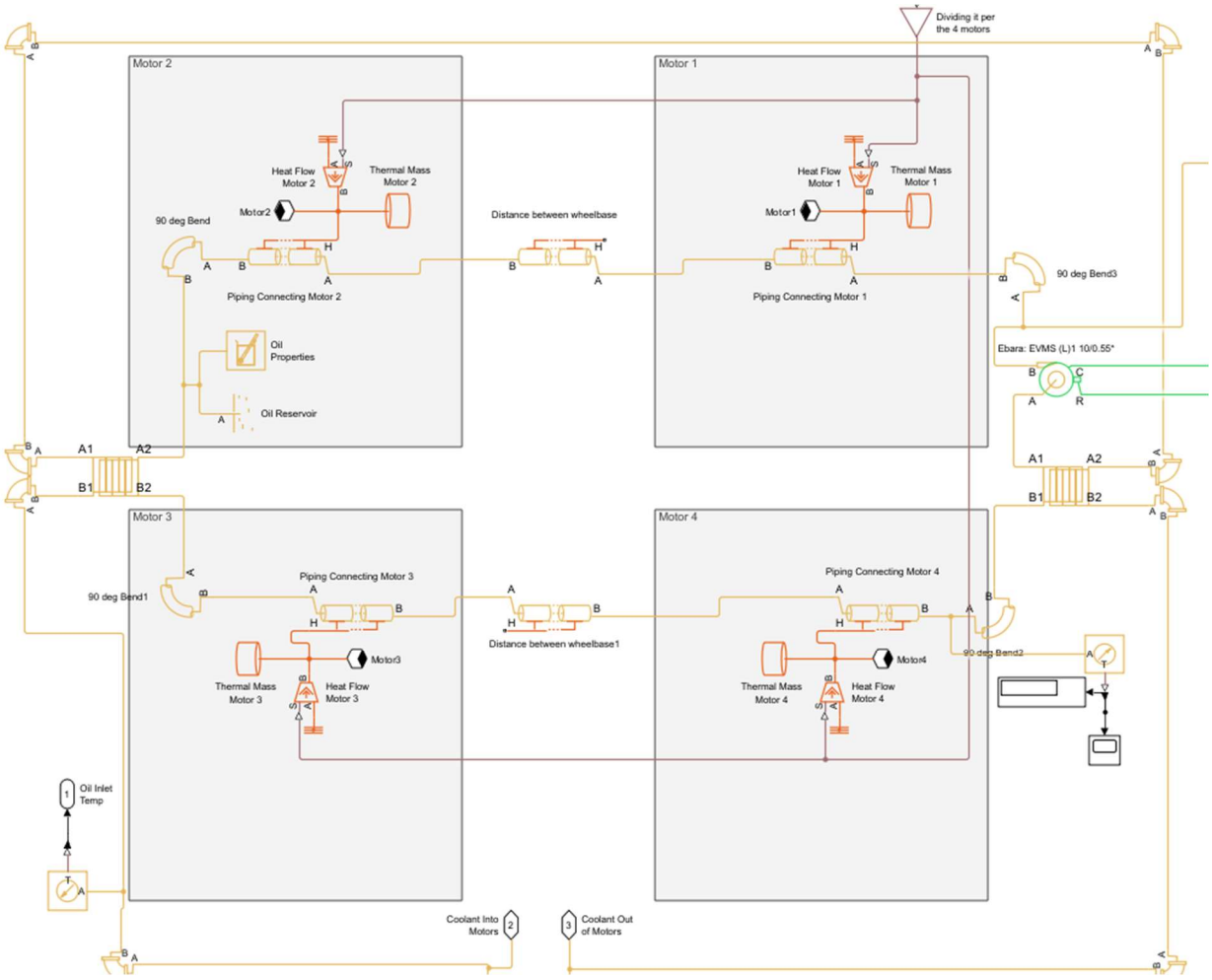


Figure 43: Motor & Coolant Connection

**Conclusion:**

After running the simulation over the 12-hour period, it was found that the uphill climb was a bigger problem than anticipated. Throughout the iterations performed, multiple resizing of all components was done to help as much as possible with their temperatures but failed to keep all components within their temperature limits during the incline.

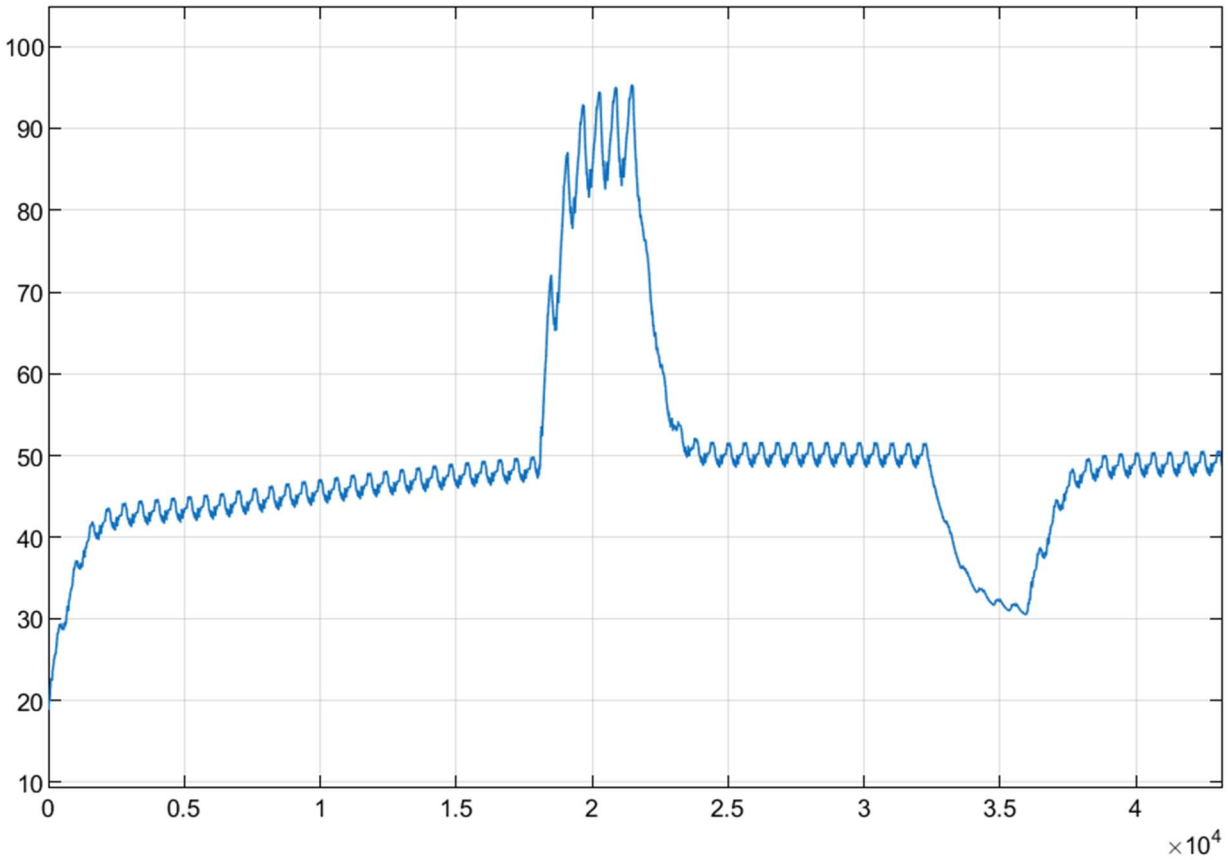


Figure 44: Battery Temperature (°C)

The battery overs around the 45°C temperature limit until the incline starts, at which is goes over to double the temperature limit near 95°C and does not recover within the temperature limit until the downhill portion.

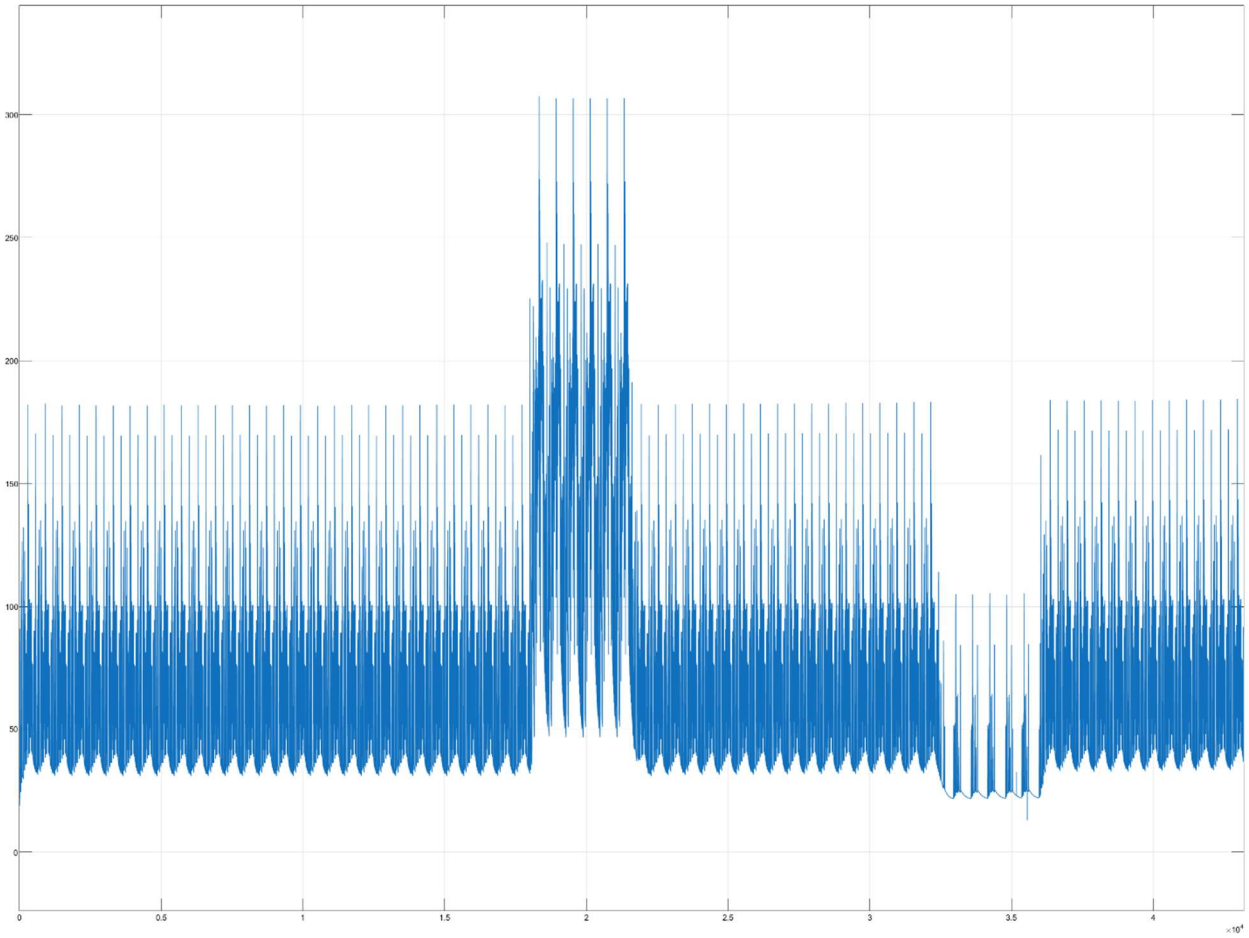

Figure 45: Inverter Temperature (°C)

For the inverter, the temperature limit was consistently surpassed throughout the drive cycle, but this was due to the almost non-existent thermal mass associated with IGBT's in the thermal system. Because of the very small mass, the temperature profile matched closely with the power profile, and as seen, the concentration of the temperature hovered under 100°C, with the only time the concentration spiking being during the uphill climb.

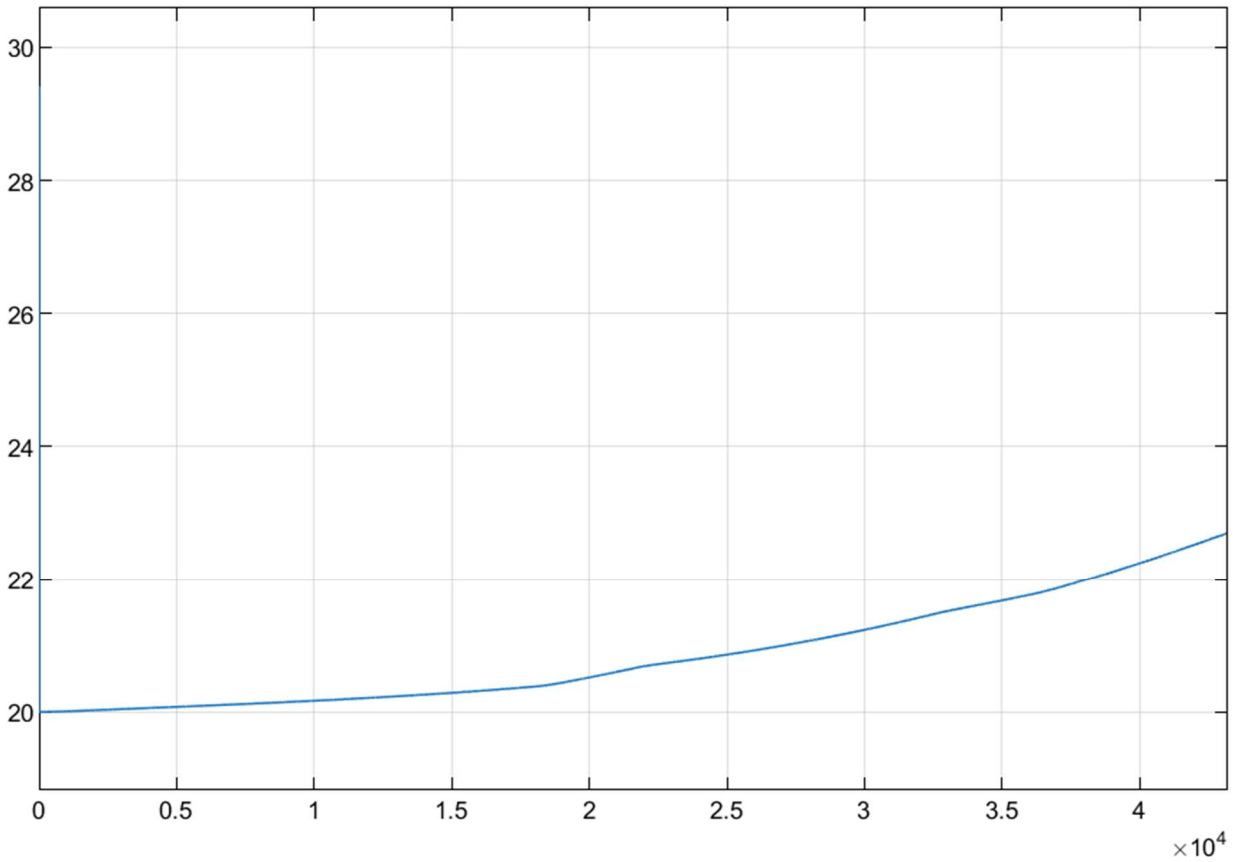


Figure 46: Coolant Inlet Temperature for Inverter (°C)

The coolant inlet temperature limit for the inverter was not a problem, as the radiator was effective in its heat rejection that we were much lower than the needed 50°C temperature.

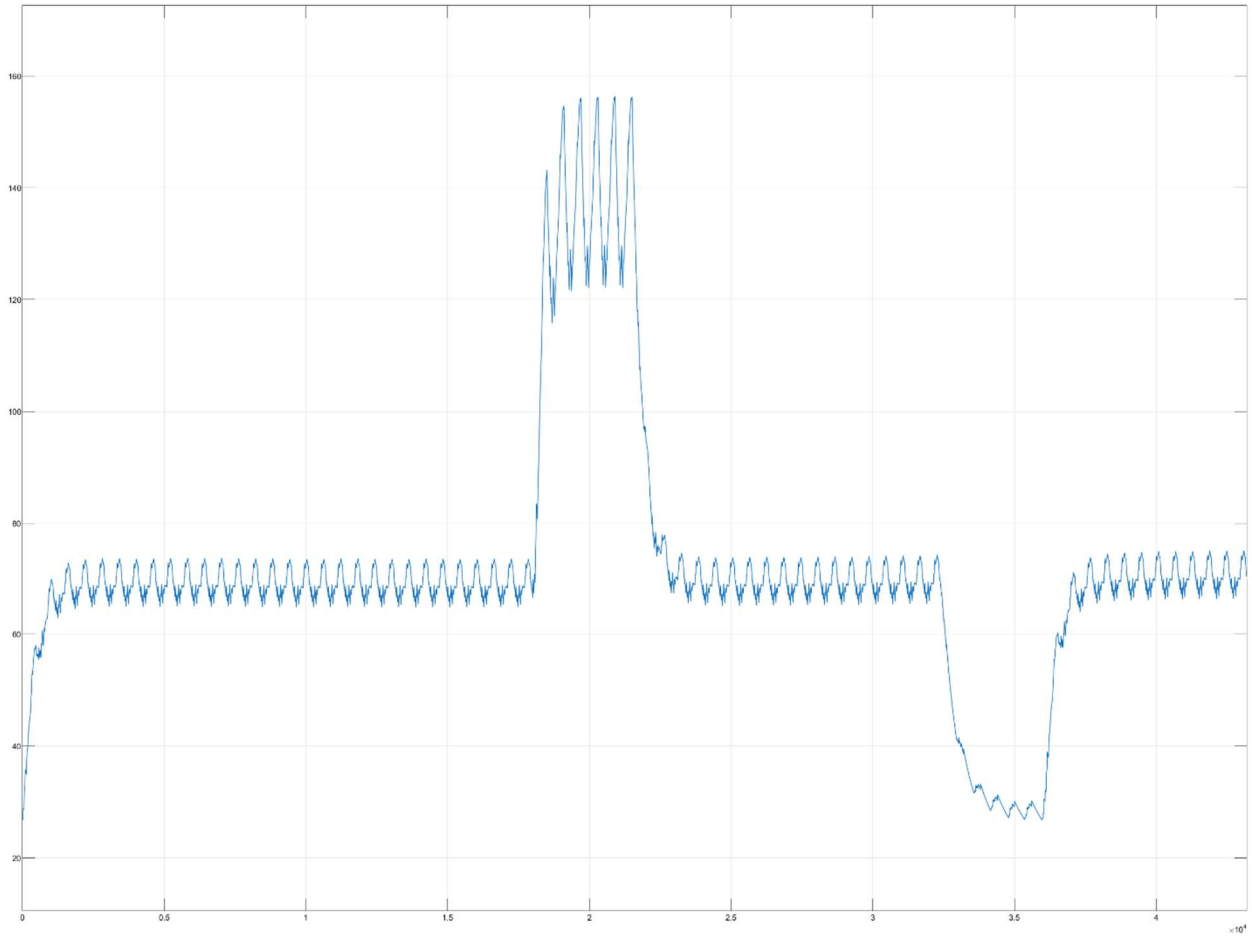

Figure 47: Motor Temperature (°C)

For the motors, the uphill portion of the drive once again proved to be a problem. With a temperature limit of 100°C, the motors were able to hover at just below 80°C throughout the duration of the drive. For the incline, the temperature did manage to spike to just under 160°C, before settling down again at just under 80°C.

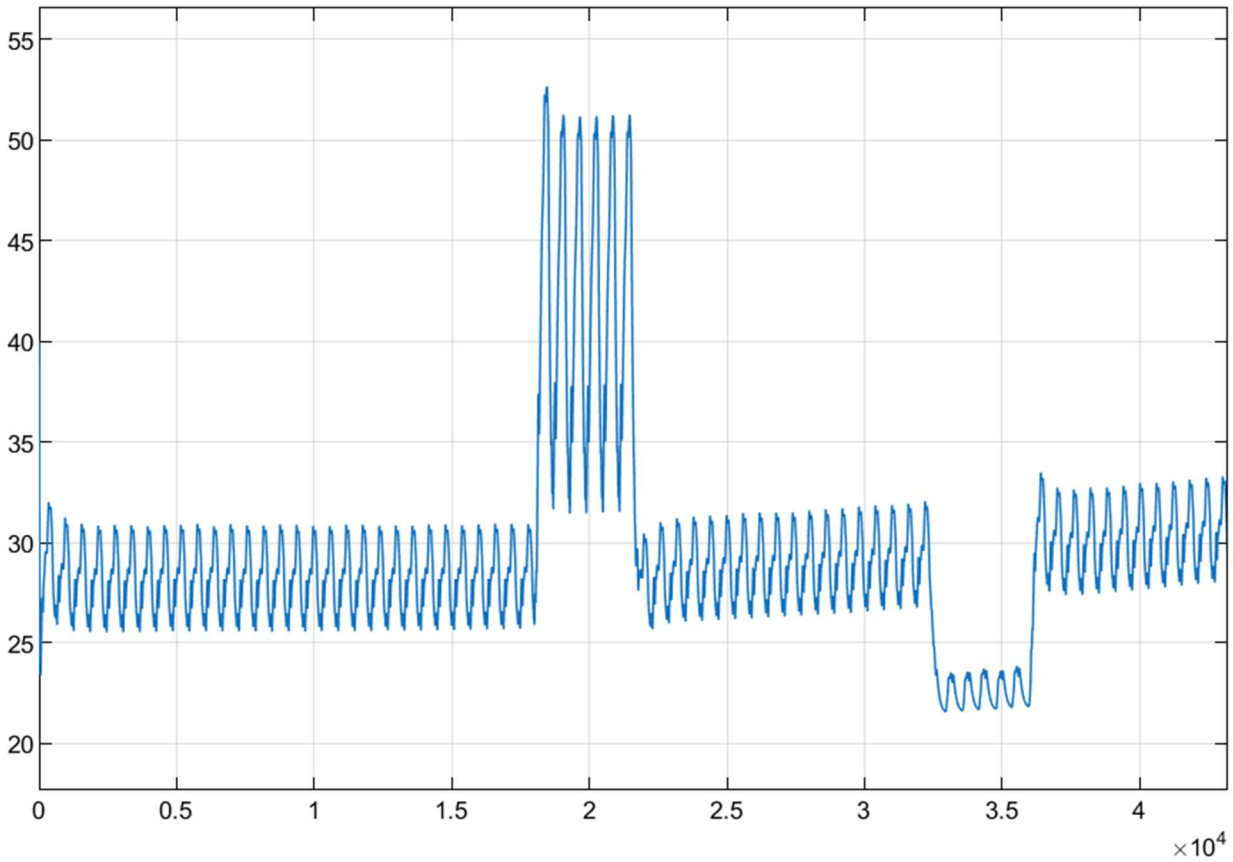


Figure 48: Transmission Oil Temperature (°C)

For the transmission oil, an inlet temperature limit of 90°C was imposed to assist with the longevity of the oil, and as seen from the figure above, the oil at the inlet of the motors reached a peak temperature of just under 55°C. This is thanks to the dual plate heat exchangers, as the oil would only have to handle two motors at a time before it reaches a heat exchanger and transfer its heat to the coolant.

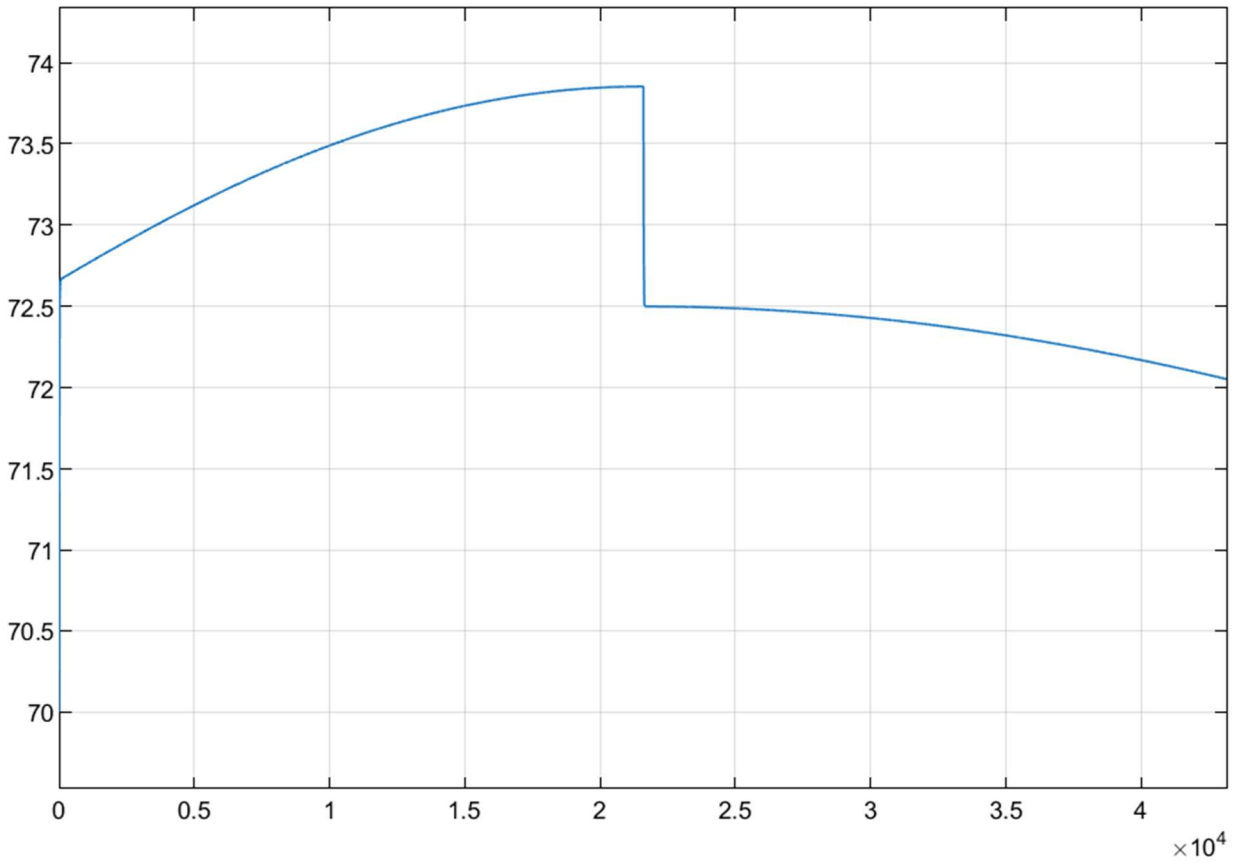


Figure 49. L Cabin Temperature (°F)

Lastly, the cabin air temperature was successfully maintained at 70°F with reasonable margin.

For future improvements, the main goal should be to focus on the incline of the power profile. It proved to be a challenge to size to account for the increase in power during that one hour, while also keeping sizes reasonable for a car. Possible solutions include pumps being driven by the shaft speed, so when the car travels at faster speeds, the pumps speed up in unison as well instead of at a constant speed throughout the drive cycle.

**References:**


[1] "California Climate, Weather By Month, Average Temperature (United States) - Weather Spark." Accessed: May 19, 2025. [Online]. Available: https://weatherspark.com/countries/US/CA#google_vignette

[2] "Los Angeles Climate, Weather By Month, Average Temperature (California, United States) - Weather Spark." Accessed: May 19, 2025. [Online]. Available: https://weatherspark.com/y/1705/Average-Weather-in-Los-Angeles-California-United-States-Year-Round

[3] O. US EPA, "Dynamometer Drive Schedules." Accessed: May 20, 2025. [Online]. Available: https://www.epa.gov/vehicle-and-fuel-emissions-testing/dynamometer-drive-schedules

[4] "EVE 3.65V 50.5Ah lithium nmc pouch battery cell," Evlithium. Accessed: May 20, 2025. [Online]. Available: https://www.evlithium.com/nmc-battery/d21-50ah-lithium-pouch-battery-cell.html

[5] "Electric-Vehicle Battery Basics," Car and Driver. Accessed: May 20, 2025. [Online]. Available: https://www.caranddriver.com/features/a43093875/electric-vehicle-battery/

[6] "50-3186NC.pdf." Accessed: May 20, 2025. [Online]. Available: https://epoxies.com/wp-content/uploads/2022/05/50-3186NC.pdf

[7] Nigel, "Specific Heat Capacity of Lithium Ion Cells," Battery Design. Accessed: May 20, 2025. [Online]. Available: https://www.batterydesign.net/specific-heat-capacity-of-lithium-ion-cells/

[8] N. Connor, "Glass | Density, Heat Capacity, Thermal Conductivity," Material Properties. Accessed: May 19, 2025. [Online]. Available: https://material-properties.org/glass-density-heat-capacity-thermal-conductivity/

[9] "How thick is the glass in a windshield? | Glass USA." Accessed: May 19, 2025. [Online]. Available: https://glassusa.com/faq/how-thick-is-the-glass-in-a-windshield/

[10] "Reflectivity in Physics and Engineering." Accessed: May 19, 2025. [Online]. Available: https://www.samaterials.com/blog/reflectivity-in-physics-and-engineering.html

[11] "Met - Human Metabolic Rates." Accessed: May 19, 2025. [Online]. Available: https://www.engineeringtoolbox.com/met-metabolic-rate-d_733.html

[12] "2025 Ford Transit® Cargo Van | Model Details & Specs | Ford.com," Ford Motor Company. Accessed: May 19, 2025. [Online]. Available: https://www.ford.com/commercial-trucks/transit-cargo-van/2025/models/transit-van/

[13] "HVAC Ducts - Air Velocities." Accessed: May 19, 2025. [Online]. Available: https://www.engineeringtoolbox.com/duct-velocity-d_928.html

[14] Y. Shin, T. Kim, A. Lee, and H. Cho, "Performance Characteristics of Automobile Air Conditioning Using the R134a/R1234yf Mixture," *Entropy*, vol. 22, no. 1, p. 4, Dec. 2019, doi: 10.3390/e22010004.

[15] I. H. Bell, J. Wronski, S. Quoilin, and V. Lemort, "Pure and Pseudo-pure Fluid Thermophysical Property Evaluation and the Open-Source Thermophysical Property Library CoolProp," *Ind. Eng. Chem. Res.*, vol. 53, no. 6, pp. 2498–2508, Feb. 2014, doi: 10.1021/ie4033999.

[16] H. Lee, *Thermal Design: Heat Sinks, Thermoelectrics, Heat Pipes, Compact Heat Exchangers, and Solar Cells*, 1st ed. Wiley, 2010. doi: 10.1002/9780470949979.

[17] “Radiator Fans - In Depth Explanation and Information,” Verus Engineering. Accessed: May 19, 2025. [Online]. Available: https://www.verus-engineering.com/blog/informative-8/radiator-fans-in-depth-explanation-and-information-32
[18] [Online]. Available: https://www.infineon.com/dgdl/Infineon-IKW15N120H3-DataSheet-v01_10-EN.pdf?fileId=db3a304325305e6d01258df9167d3741
[19] “Buy Arctic Silver ARCTIC SILVER 5 Thermally conductive paste 8.9 W/mK 3.5 g Max. temperature: 130 °C | Conrad Electronic.” Accessed: May 20, 2025. [Online]. Available: https://www.conrad.com/en/p/arctic-silver-arctic-silver-5-thermally-conductive-paste-8-9-w-mk-3-5-g-max-temperature-130-c-150352.html
[20] “Tesla Model 3 motor unit,” EV Europe. Accessed: May 19, 2025. [Online]. Available: https://eveurope.eu/en/product/tesla-model-3-motor-unit/
[21] gpienta, “What Piping Materials and Sizing Methods Are Suitable for Bulk Grease and Motor Oil Systems?,” ASPE Pipeline. Accessed: May 19, 2025. [Online]. Available: https://aspe.org/pipeline/what-piping-materials-and-sizing-methods-are-suitable-for-bulk-grease-and-motor-oil-systems/